

AD-A097 032 AIR FORCE WRIGHT AERONAUTICAL LABS WRIGHT-PATTERSON AFB OH F/G 20/5
ANALYSIS AND DESIGN OF A SUPERSONIC RADIAL OUTFLOW SYSTEM.(U)
OCT 80 S H HASINGER

UNCLASSIFIED AFWAL-TR-80-3028

NL

1 of 1
6/10/80

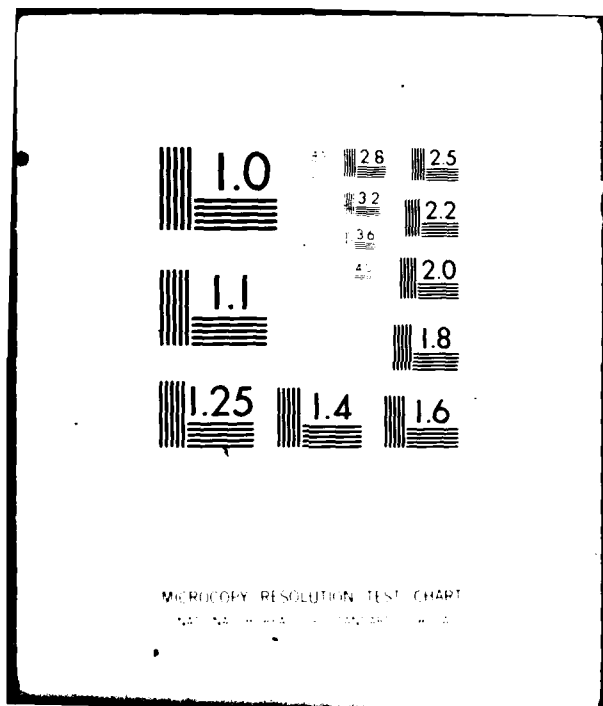
END

DATE

FILED

4-8-81

DTIC



AFWAL-TR-80-3028 ✓

LEVEL II



2

AD A 097032

ANALYSIS AND DESIGN OF A SUPERSONIC RADIAL
OUTFLOW SYSTEM

Siegfried H. Hasinger
Thermomechanics Branch
Aero Mechanics Division

DTIC
ELECTE
MAR 30 1981
D
E

October 1980

TECHNICAL REPORT AFWAL-TR-80-3028

Interim Report for Period November 1977 - November 1978

Approved for public release; distribution unlimited.

DTIC FILE COPY

FLIGHT DYNAMICS LABORATORY
AIR FORCE WRIGHT AERONAUTICAL LABORATORIES
AIR FORCE SYSTEMS COMMAND
WRIGHT-PATTERSON AIR FORCE BASE, OHIO 45433


81 3 30 071

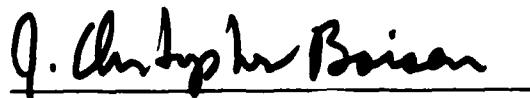
NOTICE

When Government drawings, specifications, or other data are used for any purpose other than in connection with a definitely related Government procurement operation, the United States Government thereby incurs no responsibility nor any obligation whatsoever; and the fact that the government may have formulated, furnished, or in any way supplied the said drawings, specifications, or other data, is not to be regarded by implication or otherwise as in any manner licensing the holder or any other person or corporation, or conveying any rights or permission to manufacture use, or sell any patented invention that may in any way be related thereto.

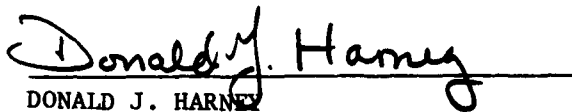
This report has been reviewed by the Office of Public Affairs (ASD/PA) and is releasable to the National Technical Information Service (NTIS). At NTIS, it will be available to the general public, including foreign nations.

This technical report has been reviewed and is approved for publication.


SIEGFRIED H. HASINGER
Aerosp Engr, Thermomechanics Branch
Aeromechanics Division


J. CHRISTOPHER BOISON
Chief, Thermomechanics Branch
Aeromechanics Division

FOR THE COMMANDER


DONALD J. HARNEY
Assistant for Experimental Simulation
Aeromechanics Division
Flight Dynamics Laboratory

"If your address has changed, if you wish to be removed from our mailing list, or if the addressee is no longer employed by your organization please notify AFWAL/FIME, W-PAFB, OH 45433 to help us maintain a current mailing list".

Copies of this report should not be returned unless return is required by security considerations, contractual obligations, or notice on a specific document.

SECURITY CLASSIFICATION OF THIS PAGE (When Data Entered)

REPORT DOCUMENTATION PAGE		READ INSTRUCTIONS BEFORE COMPLETING FORM
1. REPORT NUMBER AFWAL-TR-80-3028	2. GOVT ACCESSION NO. AD-488703	3. RECIPIENT'S CATALOG NUMBER
4. TITLE (and Subtitle) ANALYSIS AND DESIGN OF A SUPERSONIC RADIAL OUTFLOW SYSTEM		5. TYPE OF REPORT & PERIOD COVERED Interim Report November 1977 - November 1978
7. AUTHOR(s) Siegfried H. Hasinger		6. PERFORMING ORG. REPORT NUMBER
9. PERFORMING ORGANIZATION NAME AND ADDRESS Flight Dynamics Laboratory (AFWAL/FIME) Air Force Wright Aeronautical Laboratories, AFSC Wright-Patterson Air Force Base, Ohio 45433		8. CONTRACT OR GRANT NUMBER(s)
11. CONTROLLING OFFICE NAME AND ADDRESS		10. PROGRAM ELEMENT, PROJECT, TASK AREA & WORK UNIT NUMBERS Project 2307 Task 2307N4 Work Unit 2307N435
		12. REPORT DATE October 1980
		13. NUMBER OF PAGES 71
14. MONITORING AGENCY NAME & ADDRESS (if different from Controlling Office)		15. SECURITY CLASS. (of this report) Unclassified
		15a. DECLASSIFICATION/DOWNGRADING SCHEDULE N/A
16. DISTRIBUTION STATEMENT (of this Report) Approved for public release; distribution unlimited.		
17. DISTRIBUTION STATEMENT (of the abstract entered in Block 20, if different from Report)		
18. SUPPLEMENTARY NOTES		
19. KEY WORDS (Continue on reverse side if necessary and identify by block number) Supersonic Radial Diffuser Radial Outflow Laser Supersonic Radial Outflow System Cylindrical Source Laser Ring Nozzle Analysis Ring Nozzle Design		
20. ABSTRACT (Continue on reverse side if necessary and identify by block number) The design and performance of a radial outflow expansion system is presented. This information is needed for building and operating an experimental radial flow system for cold flow testing of radial diffusers of the type used in high energy radial flow laser systems. In particular, design charts for ring nozzle systems for operation with various gases are developed and effective exit Mach numbers of ring nozzle expansion systems are determined. Some considerations are given to the design of a multi-channel radial diffuser to be tested in the here designed radial flow expansion system.		

DD FORM 1 JAN 73 1473 EDITION OF 1 NOV 65 IS OBSOLETE

SECURITY CLASSIFICATION OF THIS PAGE (When Data Entered)

FOREWORD

This report covers theoretical work on supersonic radial outflow systems for investigating radial flow diffusers, carried out under Work Unit No. 2307N435 of Project No. 2307 in the Thermomechanics Branch, Aeromechanics Division, Flight Dynamics Laboratory, from November 1977 to November 1978.

Accession For	
NTIS GRA&I	<input checked="checked" type="checkbox"/>
DTIC TAB	<input type="checkbox"/>
Unannounced	<input type="checkbox"/>
Justification	
By	
Distribution/	
Availability Codes	
Avail and/or	
Dist	Special
A	

TABLE OF CONTENTS

SECTION	PAGE
I INTRODUCTION	1
II RING NOZZLE DESIGN	2
1. Description of the Nozzle System	2
2. Derivation of the Ring Nozzle Design Equations	3
3. Numerical Evaluation of the Design Equations	7
4. Discussion of the Ring Nozzle Design Chart	7
5. Design Examples	9
III Ring Nozzle Performance Analysis	14
1. General Considerations	14
2. Derivation of the Performance Equations	15
3. The Wall Force Parameter	20
4. Flow Divergence	22
IV WALL FRICTION LOSSES IN AN EXPANSION NOZZLE	24
1. General Considerations	24
2. Characteristic Flow Conditions for Wall Friction Losses	24
3. Non-Circular Expansion Nozzle	26
4. Wall Friction Coefficient for an Expansion Nozzle	28
V Theoretical Performance of a Radial Outflow System	32
1. General Aspects	32
2. Performance Calculations	32
3. Accuracy of the Performance Calculations	34

TABLE OF CONTENTS (CONCLUDED)

SECTION	PAGE
VI RADIAL DIFFUSER DESIGN CONSIDERATIONS	36
1. The Multi-Channel Radial Diffuser	36
2. Specific Diffuser Design Considerations	37
3. The Straight Flow Supersonic Diffuser	38
VII CONCLUSIONS	44

LIST OF ILLUSTRATIONS

FIGURE	PAGE
1 Scheme of a Ring Nozzle Expansion System	50
2 Ring Nozzle Design Chart for Helium	51
3 Ring Nozzle Design Chart for Air	52
4 Ring Nozzle Design Chart for CO ₂	53
5 Ring Nozzle Design Chart for Freon 12	54
6 Design of a Ring Nozzle Expansion System for $M = 2.3$	55
7 Scheme of a Radial Outflow System	56
8 Deflection of the Radial Flow into Individual Diffuser Channel	57
9 Distribution of the Wall Friction Forces Along a Supersonic Expansion Nozzle for a Constant Wall Friction Coefficient	58
10 Diffuser Plate Design for a Supersonic Multi-Channel Radial Diffuser	59
11 Wall Contour and Cross-Sectional Area for Two Different Radial Diffuser Inlet Geometries	60
12 Inlet and Exit E-Function According to Equation 80 for a Diverging Diffuser Channel	61
13 Inlet and Exit E-Function According to Equation 80 for a Constant Area Diffuser Channel	62
14 Inlet and Exit E-Function According to Equation 80 for a Converging Diffuser Channel	63

SECTION I

INTRODUCTION

A preferred flow arrangement for airborne high energy lasers is one in which the working medium flows radially outward from a centrally located and cylindrically shaped source. The individual flow elements in this arrangement are a bank of radial expansion nozzles, an annular laser cavity, and a supersonic radial diffuser. This radial flow system is, in particular, characterized by an axial length-to-diameter (L/D) ratio which is many times larger than that of commonly known radial diffusers such as those used in turbomachines. This large relative length introduces complications for the design of such systems. Particular difficulties in this respect are encountered with the design of the diffuser.

This report describes the design of a cold flow radial flow system for investigating radial diffusers for laser applications. The radial flow feature requires the design of special flow expansion units, which in the present case consist of "ring" nozzles (Figure 1). In the first part of this report, a special design procedure for these nozzles is developed. To produce the radial flow field applicable to radial flow lasers the expansion must take place in a multiplicity of nozzles. The subdivision of the flow into small units introduces flow losses which can no longer be accounted for by a simple expansion efficiency. In the second part of the report, a careful loss analysis is presented for an analytic prediction of the expansion nozzle performance. This prediction is a necessity for the present test rig design which does not allow an experimental performance determination. In the final part of the report, some basic considerations are given to the design of a multi-channel radial diffuser.

SECTION II

RING NOZZLE DESIGN

1. DESCRIPTION OF THE NOZZLE SYSTEM

The radial outflow expansion nozzles are made up of ring shaped elements forming the walls of the nozzles. They are referred to here as "ring nozzles". Figure 1 gives a scheme of a ring nozzle system.

The perforated tube in the center of the system is a device to provide uniform flow conditions along the axis of the system. By maintaining a sufficient low porosity of the tube, the pressure in the tube can be kept high and the velocities in the tube low. The necessity for such a supply tube depends primarily on the length-to-diameter ratio of the nozzle system, i.e., the larger the number of the ring nozzles the higher the pressure must be. This perforated tube arrangement is a specific feature of the present model.

For an actual laser, either due to heat addition in the nozzle system (chemical laser) or due to very high expansion Mach numbers (gas dynamic laser) nozzle configurations result, which in general do not require the use of a high pressure supply tube to arrive at uniform flow conditions. The present experimental investigations deal with the comparatively low Mach numbers of the chemical lasers ($M = 2$ to 3), use cold air as operating medium, i.e., no heat addition, and contemplate testing large length to diameter systems ($\frac{L}{2R} \rightarrow 3$). All these conditions make the perforated supply tube an absolute necessity.

First, equations will be derived which relate the nozzle dimensions indicated in Figure 1 to the fluid-dynamic and thermodynamic conditions of the flow system. These equations are then used for the preparation of ring nozzle design charts.

2. DERIVATIONS OF THE RING NOZZLE DESIGN EQUATIONS

The following magnitudes enter the ring nozzle design (for geometric data see Figure 1):

Flow conditions:

Mach number M
 Reynolds number Re^* (at throat)
 Mass flow rate W

Thermodynamic conditions:

Plenum pressure P_0
 Plenum temperature T_0
 Ratio of spec. heats γ
 Gas constant R_G
 Absolute viscosity μ^* (at throat)

Geometric conditions:

R
 H
 α
 R/r
 H/h
 R/H
 $L/(2R)$

With above-listed magnitudes, five equations can be formed with R/r and H/h appearing explicitly in all equations. Using these two ratios as coordinates of a graphic display of the relations, all magnitudes necessary for a ring nozzle design can be represented in one diagram (design chart) as shown in Figures 2 through 5 for a number of different gases. The five relations are derived below. They are listed in terms of the pertinent curve parameter.

a. Mach number

From continuity

$$\frac{A}{A^*} = \frac{2R\pi H}{2r\pi h} = \frac{R \cdot H}{r \cdot h} \quad (1)$$

with the well known relation for the area expansion ratio in isentropic flow we obtain the first equation

$$\left(\frac{R}{r}\right) \left(\frac{H}{h}\right) = \frac{1}{M} \left[\frac{1 + \frac{\gamma-1}{2} M^2}{\frac{\gamma+1}{2}} \right]^{\frac{\gamma+1}{2(\gamma-1)}} \quad (2)$$

For given gas, i.e., for a given γ , this relation can be plotted in the design chart with the Mach number as parameter.

b. $(R/H) \operatorname{tg} \alpha$

From Figure 1 we find

$$\operatorname{tg} \alpha = \frac{\frac{H-h}{2}}{R-r} = \frac{1 - \frac{h}{H}}{2\left(\frac{R}{H} - \frac{r}{H}\right)} \quad (3)$$

with some rearrangement we obtain the second design equation

$$\frac{H}{h} = \frac{\frac{R}{r}}{\frac{R}{r} - 2 \frac{R}{H} \operatorname{tg} \alpha \left[\frac{R}{r} - 1 \right]} \quad (4)$$

This relation is plotted in the design chart with $(R/H) \operatorname{tg} \alpha$ as parameter.

c. $(R/W) \operatorname{Re}^*$

Continuity yields

$$W = A^* \rho^* v^* \quad (5)$$

with

$$A^* = 2\pi r \cdot h \quad (6)$$

$$\operatorname{Re}^* = \frac{v^* \cdot h \cdot \rho^*}{\mu^*} \quad (7)$$

Equation 5 becomes

$$W = 2r\pi\mu^*Re^* \quad (8)$$

multiplying both sides by R we obtain as third equation after some rearrangement

$$\frac{R}{r} = 2\pi\mu^* \left[\frac{R}{W} Re^* \right] \quad (9)$$

For a given gas, i.e., a given μ^* , the expression $(R/W)Re^*$ is proportional to R/r and can be plotted along the R/r axis in the design chart.

$$d. (P_0 H) / (\sqrt{T_0} Re^*)$$

The continuity relation given by Equation 5 can be developed in a different way by using the equation of state

$$\rho^* = \frac{P^*}{R_G T^*} = \frac{P_0}{R_G T_0} \cdot \frac{T_0 P^*}{T^* P_0} \quad (10)$$

and the equation for the sonic speed

$$v^* = \sqrt{R_G T^* \gamma} \quad (11)$$

Using these two equations, Equation 5 becomes

$$W = A^* \left[\frac{P^*}{P_0} \sqrt{\frac{T_0}{T^*} \frac{\gamma}{R_G}} \right] \frac{P_0}{\sqrt{T_0}} \quad (12)$$

The expression in brackets is a unique function of the gas properties. It will be brought into a convenient form for evaluation. Considering sonic conditions in the throat

$$\frac{T}{T^*} = 1 + \frac{\gamma-1}{2} \quad (13)$$

$$\frac{P}{P^*} = \left(1 + \frac{\gamma-1}{2} \right)^{\frac{\gamma}{\gamma-1}} \quad (14)$$

the expression in brackets can be written

$$\left[\frac{p^*}{p_o} \sqrt{\frac{T_o}{T^*} \frac{\gamma}{R_g}} \right] = \sqrt{\frac{1}{(1 + \frac{\gamma-1}{2}) \frac{\gamma+1}{\gamma-1}}} \sqrt{\frac{\gamma}{R_g}} = \phi \quad (15)$$

With this substitution and using Equations 6 and 8, Equation 12 can be written

$$\mu^* Re^* = h \cdot \phi \frac{p_o}{\sqrt{T_o}} \quad (16)$$

multiplying both sides of Equation 16 by H we arrive at the fourth design equation

$$\frac{H}{h} = \left[\frac{p_o}{\sqrt{T_o}} \frac{H}{Re^*} \right] \frac{\phi}{\mu^*} \quad (17)$$

The expression in brackets is proportional to H/h for a given gas, and can be plotted along the H/h axis in the design chart. The magnitude ϕ/μ^* is a unique function of the working medium.

$$e. (p_{Ex} H r) / (T_o W)$$

Using Equation 6 and dividing both sides of Equation 12 by H and p_{Ex} this equation becomes

$$\frac{W}{p_{Ex} H} = \frac{2\pi n h}{H} \frac{p^*}{p_o} \sqrt{\frac{T_o}{T^*} \frac{\gamma}{R_g}} \frac{p_o}{\sqrt{T_o} p_{Ex}} \quad (18)$$

Using Equation 15 we arrive after some simple transformation at the fifth equation

$$\frac{H}{h} = \left[\frac{H r p_{Ex}}{W \sqrt{T_o}} \right] \phi \cdot 2\pi \frac{p_o}{p_{Ex}} \quad (19)$$

For a given gas, the ratio P_o/P_{Ex} is a sole function of the nozzle exit Mach number

$$\frac{P_o}{P_{Ex}} = \left[1 + \frac{\gamma-1}{2} M^2 \right]^{\frac{\gamma}{\gamma-1}} \quad (20)$$

According to the area relation for a supersonic nozzle (Equation 2), Mach number, M , in Equation 20 and consequently the pressure ratio in Equation 19 are both, for a given gas, sole functions of the coordinate values of the design chart. Thus, Equation 19 can be entered into the design chart with the expression in brackets appearing as parameter, ϕ being also a unique function of the gas properties.

3. NUMERICAL EVALUATION OF THE DESIGN EQUATIONS

The equations derived above have been evaluated for four different gases and the results are plotted in Figures 2 through 5. The following consistent set of dimensions has been used for the evaluation of the design equations:

W	Kg/sec	T	°K
H	m	R_G	Newton m/(Kg °K)
P	Newton/m ²	μ	Newton sec/m ²
R	m		

The required properties of the here considered gases are listed in Table 1. Included in the table are expressions which occur in Equations 9, 15, 17, and 19 and are derived from the properties. The listed absolute viscosity values apply only to near ambient gas temperatures.

4. DISCUSSION OF THE RING NOZZLE DESIGN CHARTS

The design charts in Figures 2 through 5 apply to four different gases. A point in any of the charts fixes the geometric design of a ring nozzle unit for the indicated gas as working medium. To fix the design point

itself, either its coordinates, two curve parameters, or one of its coordinates and one parameter must be given. Examples for designing ring nozzle systems will be shown in Section II.

Two limiting conditions for the ring nozzle design can be directly recognized from the design charts.

a. For a multi-ring nozzle system, the value of H/h should not be much lower than 2; otherwise the subsonic approach Mach number to the nozzle becomes too high. This is obvious from Figure 1 which shows that in a stack of nozzles the subsonic flow cross section available is limited by the value of H/h . For instance, for $H/h = 2$, the subsonic Mach number at the inlet to the nozzle ring can never be smaller than 0.3 in case of air. To obtain uniform flow conditions in the ring nozzle system, a low subsonic approach Mach number is desirable or extra measures must be taken to provide a uniform flow approaching the nozzle throat (Section II).

b. Limiting conditions are also introduced by the values which are desired for the parameter $(R/H)\tan\alpha$. Values for α should be about 10° , i.e., $\tan\alpha$ should be about 0.2. R is in general several times larger than H , say 4 times. Thus, $(R/H)\tan\alpha$ will be typically about 0.8. Thus the upper left hand and lower right hand corners of the design charts are generally undesirable regions for ring nozzle operations.

In general, the charts show that nozzles for low supersonic Mach numbers, say at least below 2, are difficult to design. Comparing Figure 2 to Figure 5, where each figure is made up for a different gas, one recognizes that the difficulties are eased with gases having a low γ such as CO_2 or Freon.

In principle, there is a ring nozzle possible with $\alpha = 0^\circ$ and consequently $H/h = 1$, i.e., the nozzle walls are parallel. As the charts show, very large radius ratios R/r are necessary to obtain high Mach numbers in this case. Such a parallel wall expansion system still requires a throat section for the transition from subsonic to supersonic flow.

For a large axial length-to-diameter expansion system where the flow must be subdivided into small expansion units to assure a uniform approach flow to the system, the parallel wall arrangement affects the ring nozzle design in a special way. Where the throat contour changes to the parallel wall contour, a subdivision of the flow is no longer necessary since parallel walls in the flow serve no useful purpose in this case. Thus, the ring nozzle system or any other type of subdivision is reduced to an array of very short nozzles. In the extreme, the throat section may be only a perforated tube. Due to the inherent requirement for a throat the angle α as defined in Figure 1 can never be zero in a multi-nozzle arrangement.

The contour of a nozzle ring between throat and exit is not specified in this design procedure. The angle α relates only the location of the exit edge to that of the throat. One can think of a nozzle contour where the flow expansion is made very strong immediately after the throat, as actually done for short, highly efficient nozzles, with the outer portion of the nozzle rings ending into parallel walls. Similar to the reduced nozzle system explained above, these parallel portions could again be eliminated without affecting the expansion process. Thus, the design charts give the nozzle Mach number at a radius derived from the angle α and not necessarily given by the nozzle exit edge.

5. DESIGN EXAMPLES

For the experimental flow model for which the present design study has been initiated as mentioned in Section I, a Mach number 2.3 and a Mach number 3.3 nozzle system for air as operating medium were designed. The design process followed in these cases will be given here.

a. M 3.3 nozzle system

Fixed conditions for this system were:

$L/(2R)$	= 3	(given condition)
W_{tot}	= 9 Kg/sec	(limit of air supply)
T_o	= 293°K	(test stand design)

REFAL IR 80-3028

Desirable conditions were:

$$n > 10$$

$$r = 0.0127 \text{ m} \quad (\text{from supply tube design})$$

$$M = 3.4$$

$$P_0 = 0.2 \text{ kg/cm}^2 = 1.962 \cdot 10^4 \text{ Newton/m}^2$$

$$H = 0.005 \text{ m} \quad (\text{large enough for flow survey})$$

$$Re = 10^5$$

For a first approach we try:

$$2R = 1.75'' = 0.0444 \text{ m}$$

$$\text{and} \quad R/r = 1.75$$

$$\text{and} \quad H = 0.005 \text{ m}$$

$$\text{and} \quad R/H = 4.44$$

$$\text{and} \quad (R/H) \tan \alpha = 0.78$$

With these, the number of ring nozzles

$$L = n \cdot H$$

$$\text{and} \quad L/(2R) = 3$$

$$\text{and} \quad n = \frac{2R}{H} \cdot 3 = \frac{0.0444}{0.005} \cdot 3 = 26.6$$

For a straight number we choose $n = 27$

the weight flow per nozzle unit is

$$W = \frac{W_{\text{tot}}}{n} = \frac{9}{27} = 0.333 \text{ kg/sec}$$

Now we can determine the curve parameter

$$\frac{W}{\sqrt{T_0}} = \frac{P_{Ex}}{P_0} = \frac{0.005 \cdot 0.0254 \cdot 0.2 \cdot 9.8 \cdot 10^4}{0.333 \cdot 17.1 \cdot 2} = 0.219$$

With this value and $R/r = 1.75$ we read from the chart in Figure 3

that $R/H = 4.2$.

The actual dimensions chosen for the engineering design of the nozzle system were the following:

$$\begin{aligned}
 2R &= 1.75" &= 44.45\text{mm} &= .04445\text{m} \\
 2r &= 1.00" &= 25.40\text{mm} &= .0254\text{m} \\
 H &= .192" &= 4.877\text{mm} &= .004877\text{m} \\
 h &= .059" &= 1.499\text{mm} &= .001499\text{m} \\
 \epsilon &= 10^{-6}
 \end{aligned}$$

Only H is slightly different from the value used in the first approach.

From these chosen values follows:

$$\begin{aligned}
 R/r &= 1.75 & A/A^* &= 5.695 \\
 H/h &= 3.254 & R/H &= 4.557 \\
 M &= 3.31 & (R/H)\text{tg} \epsilon &= 0.808
 \end{aligned}$$

The other magnitudes occurring in the design chart become

$$\begin{aligned}
 \frac{P_{Ex}}{W} \frac{r}{H} \sqrt{T_0} &= 0.22 \quad \frac{\text{Newton} \cdot \text{sec}}{\text{Kg} \cdot \text{m}^2 \text{K}} \\
 \frac{R}{W} \text{Re}^* &= 1.547 \cdot 10^4 \quad \frac{\text{m} \cdot \text{sec}}{\text{Kg}} \\
 \frac{P_{0H}}{\sqrt{T_0} \text{Re}^*} &= 1.45 \cdot 10^3 \quad \frac{\text{Newton}}{\text{m}^2 \text{K}}
 \end{aligned}$$

Derived values of interest are:

$$\begin{aligned}
 \frac{P_{Ex}}{W} &= 0.22 \quad \frac{\sqrt{T_0}}{r \cdot H} = 60701 \quad \frac{\text{Newton} \cdot \text{sec}}{\text{m}^2 \text{Kg}} \\
 &= 0.6188 \quad \frac{\text{Kg} \cdot \text{sec}}{\text{m}^2 \text{Kg}}
 \end{aligned}$$

AFWAL-TR-80-3028

for example, for $P_{Ex} = 0.2 \text{ Kg/m}^2$

it is $W = \frac{0.2}{0.6188} = 0.323 \text{ Kg/sec}$

For the nozzle throat Reynold number, we obtain

$$\begin{aligned} Re^* &= 1.547 \cdot 10^4 \cdot \frac{W}{R} \\ &= 2.25 \cdot 10^5 \end{aligned}$$

The nozzle system in Figure 1 is drawn in proportion to the designs presented above.

b. M 2.3 Nozzle System

This system was intended to have the same outside diameter and nozzle spacing as the high Mach number nozzle system.

Thus, the following magnitudes are fixed:

$$2R = 0.0444 \text{ m}$$

$$H = 0.00488 \text{ m}$$

$$R/H = 4.557$$

Given by the test facility: $T_0 = 293^\circ \text{ K}$

For magnitudes which can be freely chosen the following desirable ranges were established:

$$\alpha = 10^\circ \text{ to } 15^\circ$$

$$R/r > 1.2$$

$$H/h > 1.5$$

$$M < 2.3$$

It follows that $(R/H)\tan\alpha = 0.803 \text{ to } 1.222$

Those ranges fix an area in the design chart within which the design point may be selected, as shown in Figure 3. The following coordinates were chosen for the point:

$$R/r = 1.25 \quad H/h = 1.7$$

The values of the curve parameters for the chosen point are:

$$(R/H)tg\alpha = 1.03$$

$$M = 2.265$$

$$\frac{P_{Ex} rH}{W \sqrt{T_0}} = 0.566 \quad \frac{\text{Newton sec}}{\text{Kg } ^\circ\text{K}}$$

Other derived values are:

$$tg\alpha = 0.2312$$

$$\alpha = 13.02^\circ$$

$$\frac{P_{Ex}}{W} = 156263 \frac{\text{Newton sec}}{\text{m}^2 \text{Kg}} = 1.593 \frac{\text{Kg' sec}}{\text{cm}^2 \text{Kg}}$$

for $P_{Ex} = 0.5 \text{ Kg'/cm}^2$ it is $W = 0.314 \text{ Kg/sec}$

A low Mach number ring nozzle system designed according to conditions above is shown in Figure 6. As indicated before, due to the low H/h value of 1.7, the subsonic approach Mach number is near .4 and even higher at the smaller radius where the screen is positioned. This screen serves as flow equalizer for the flow approaching the actual expansion nozzle.

SECTION III

RING NOZZLE PERFORMANCE ANALYSIS

1. GENERAL CONSIDERATIONS

Flow expansion in a supersonic nozzle is normally a very efficient process. For instance, for a Mach number 3, axis-symmetric nozzle efficiencies near 99% are possible. However, for the radial outflow system considered here, lower efficiencies must be expected due to certain geometric constraints imposed on the system. Laser applications require that the axial length of the nozzle system is several times larger than its diameter. Such shape can only be obtained by subdividing the expansion system into many small units. In the present case, this is done by a series of nozzle rings (Figure 1). This subdivision reduces the characteristic length dimensions and consequently the characteristic Reynolds number of the system. Thus, for the same flow rate, the wall friction coefficient for the radial outflow system must be higher than that for an axis-symmetric nozzle.

At the exit of the multi unit expansion system, the flow experiences a sudden flow cross-section enlargement due to the finite thickness of the nozzle exit edges. This is another cause for flow losses. Finally, the flow in a radial outflow system has an inherent divergence which leads to a momentum loss, if the flow has to be turned into the discrete directions of the channels of the radial diffuser.

The expansion losses can be determined fairly closely by analysis. This is important for the evaluation of experimental results with radial outflow systems. The end conditions of the expansion, which are the inlet condition for the diffuser cannot clearly be determined in the experiments, mainly due to the presence of the nozzle wakes in the flow.

The space between the nozzle exits and the diffuser inlet (laser cavity) is not readily accessible to instrumentation for a complete flow survey. Analytic predictions which account for possible losses during expansion are therefore more reliable than limited flow measurements.

In the following, an analytic process for calculating the performance of a ring nozzle system accounting for the expansion losses indicated above will be derived. The analysis relates the flow conditions between significant flow cross section to each other with the conservation laws for mass, momentum, and energy. The resulting equations are given in the form of force equations which allow a ready addition of the wall friction forces in terms of the common pipe friction coefficient. This method has been used previously for determining ejector performances (References 1, 2). Equations developed for the ejector case can be used here directly by setting the primary and secondary velocity equal in these equations. In Reference 2, this procedure has been already applied to the diffuser case. The derivations provided below follow very closely the outline given for the ejector case in Reference 1.

2. DERIVATION OF THE PERFORMANCE EQUATIONS

A. Momentum Equation

The momentum equation applied to the adiabatic flow in a duct, where inlet (1) and exit (2) may have different cross sectional areas, can be written in the following form:

$$m \cdot v_1 = m \cdot v_2 + F_W + F_p + F_f \quad (21)$$

F_W in this equation is the wall pressure force acting between the wall and the flow in flow direction in a non-constant area duct

$$F_W = \int_{A_2}^{A_1} (P_1 - P_W) dA \quad (22)$$

where P_W is the local wall pressure and $(dA)_W$ a differential wall area projected in flow direction.

F_p is the force acting in the fluid in flow direction within the central region where no wall pressure forces act

$$F_p = A_1 (P_1 - P_2) \quad (23)$$

F_f in Equation 21 is the wall friction force acting on the flow along the duct wall. This force may be expressed in the form used for normal pipe friction

$$F_f = A \cdot c_f \cdot \rho \cdot \frac{v^2}{2} \cdot \frac{L}{D} \quad (24)$$

where a judicious choice must be made for the reference crosssection A . The friction coefficient, c_f , in this equation applies to fully developed flow (Section IV). The fluid pressure forces and the friction forces will be discussed below in more details.

(1) Fluid Pressure Forces F_w and F_p

Both forces have the same cause, which is the pressure change in flow direction. They are best treated together. Following procedures given in Reference 1, Equation 22 is written in a form which facilitates the integration of this equation by introducing a shape factor i . All equations are also written in a form consistent with the ejector case. For this reason Equation 23 does not appear explicitly in the following derivations. In this way, the wall pressure forces become

$$F_w = (A_1 - A_2) \frac{P_1 - P_2}{2} i \quad (25)$$

Then for the total fluid pressure forces one can write

$$F_{w+p} = - \left[(A_1 - A_2) \frac{P_1 - P_2}{2} i + A_2 (P_1 - P_2) \right] \quad (26)$$

by using the abbreviation:

$$t = \frac{A_2}{A_1} \quad (27)$$

Equation 26 can be transformed into

$$F_{W+P} = (p_2 - p_1)A_2\left(\frac{i}{2t} + 1 - \frac{i}{2}\right) \quad (28)$$

Writing

$$\tau = \frac{i}{2t} + 1 - \frac{i}{2} \quad (29)$$

the final form of the fluid pressure forces becomes

$$F_{W+P} = \tau \cdot t \cdot p \cdot A_1 \left(\frac{p_2}{p_1} - 1 \right) \quad (30)$$

(2) Wall Friction Force

The use of the pipe friction coefficient for expressing friction forces requires the selection of a reference cross section together with the flow velocity in this cross section. For a normal pipe, the reference conditions are those at the inlet of the pipe. As will be shown in Section IV, in the present case the conditions at the duct exit are a particularly useful choice.

Considering

$$\rho_2 v_2^2 = p_2 \gamma M_2^2 \quad (31)$$

we can write for the friction forces with Equation 24

$$F_f = A_2 \cdot c_f \cdot p_2 \cdot \gamma \cdot M_2^2 \frac{L}{2D} \quad (32)$$

(3) Final Momentum Equation

Expressing the flow momentum in Equation 21 by

$$m \cdot v = A \cdot p \cdot \gamma \cdot M^2 \quad (33)$$

and using above developed expressions for fluid pressure forces and wall friction forces, Equation 21 becomes

$$A_1 p_1 \gamma M_1^2 = A_2 p_2 \gamma M_2^2 + \tau \cdot t \cdot p_1 \cdot A_1 \left(\frac{p_2}{p_1} - 1 \right) + A_2 c_f p_2 \gamma M_2^2 \frac{L}{2D} \quad (34)$$

This equation can be readily transformed into

$$\frac{\gamma M_1^2}{t} + \tau = \frac{p_2}{p_1} \left[\gamma M_2^2 \left(\frac{c_f L}{2D} + 1 \right) + \tau \right] \equiv B \quad (35)$$

Equation 35 is valid for any adiabatic change of state in a duct with varying cross-section areas such as flow expansion in a nozzle, sudden change in flow cross-section, or supersonic diffusion in a constant area duct. The differentiation between these various possible changes appears only in the wall force parameter τ . The determination of τ will be shown in Section III.

Equation 35 yields the pressure ratio across the duct

$$\frac{p_2}{p_1} = \frac{B}{\gamma M_2^2 \left(\frac{c_f L}{2D} + 1 \right) + \tau} \quad (36)$$

The duct exit Mach number on the right side is still unknown. We obtain this Mach number from the requirement for conservation of mass and energy in the flow, as shown below.

b. Mass and Energy Equation

From continuity, follows

$$m = v_1 \cdot A_1 \cdot \rho_1 = v_2 \cdot A_2 \cdot \rho_2 \quad (37)$$

with

$$a = \sqrt{\gamma \cdot R \cdot T} \quad (38)$$

$$\rho = \frac{P}{RT} \quad (39)$$

$$\frac{V}{a} = M \quad (40)$$

we can write

$$\frac{M_2}{M_1} = \frac{A_1}{A_2} \frac{p_1}{p_2} \sqrt{\frac{T_2}{T_1}} \quad (41)$$

or

$$M_2 = \frac{M_1}{t} \frac{p_1}{p_2} \sqrt{\frac{T_2}{T_0} \frac{T_0}{T_1}} \quad (42)$$

For an adiabatic change of state, it is

$$\frac{T_2}{T_0} = 1 + \frac{\gamma - 1}{2} M_2^2 \quad (43)$$

Then, Equation 42 can be written

$$M_2 \left(1 + \frac{\gamma - 1}{2} M_2^2 \right)^{1/2} = \frac{M_1}{t} \frac{p_1}{p_2} \sqrt{\frac{T_0}{T_1}} \quad (44)$$

With p_1/p_2 from Equation 36, we arrive at

$$\frac{M_2 \left(1 + \frac{\gamma - 1}{2} M_2^2 \right)^{1/2}}{\gamma M_2^2 \left(\frac{c_f L}{2D} + 1 \right) + \tau} = \frac{M_1}{B \cdot t} \sqrt{\frac{T_0}{T_1}} = E \quad (45)$$

The right side of this equation is made up of magnitudes strictly given by the inlet conditions and the duct geometry in terms of t .

The left side contains only magnitudes given by the exit conditions and the factor τ which is a constant for a particular kind of duct flow.

Equation 45 can be solved for M_2

$$M_2^2 = \frac{1 - \left[\frac{+}{-} \sqrt{1 - \frac{\alpha \tau^2}{c} \left(2 \frac{c}{l} + \frac{1}{\gamma} - 1 \right) + \alpha \tau} \right]}{c \alpha \gamma - \gamma + 1} \quad (46)$$

where

$$c = 1 + \frac{c_f L}{2D} \quad (47)$$

$$\alpha = 2 \gamma E^2 c \quad (47a)$$

The positive root in this equation gives the subsonic solution for the exit Mach number and the negative root the supersonic solution if compatible with the existing conditions.

3. WALL FORCE PARAMETER

a. Expansion Nozzle

For zero wall friction, Equation 46 applied to an expansion nozzle must yield the same result as the common thermodynamic relations for an isentropic expansion. From this requirement, the factor τ can be determined for the case of an expansion nozzle. With a τ -value found in this way for a particular case of expansion nozzle, Equation 46 allows one to add friction forces to this expansion process and find the new exit conditions. This procedure to calculate flow expansion with friction is an approximate method since wall friction may change the pressure distribution along the expansion nozzle and thus the value τ of the process. There are indications that this influence on τ is in practical cases small enough in comparison to the direct influence of friction on the flow that the change of τ can be neglected. A possible approach for eliminating this influence is to calculate the flow expansion in segments small enough for the pressure distribution to become a straight line independent of the presence of wall friction. The factor τ becomes a constant in this case.

To determine τ for an isentropic expansion process, we solve Equation 34 for τ with wall friction zero

$$\tau = \frac{p_1 \gamma M_1^2 A_1 - p_2 \gamma M_2^2 A_2}{(p_2 - p_1) A_2} \quad (48)$$

or somewhat rearranged

$$\tau = \frac{\gamma \left[M_1^2 \frac{A_1}{A_2} \frac{p_1}{p_2} - M_2^2 \right]}{1 - \frac{p_1}{p_2}} \quad (49)$$

The area ratio and the pressure ratio in this equation are determined from the well known relations for isentropic expansion

$$\frac{A_1}{A_2} = \frac{M_2}{M_1} \left[\frac{1 + \frac{\gamma-1}{2} M_1^2}{1 + \frac{\gamma-1}{2} M_2^2} \right]^{2 \frac{\gamma+1}{\gamma-1}} \quad (50)$$

$$\frac{p_2}{p_1} = \left[\frac{1 + \frac{\gamma-1}{2} M_1^2}{1 + \frac{\gamma-1}{2} M_2^2} \right]^{\frac{\gamma}{\gamma-1}} \quad (51)$$

For a given gas, a given inlet Mach number and a given nozzle area ratio, τ can be determined from Equation 49 with the help of Equations 50 and 51. The value of τ changes strongly with the expansion conditions and must be determined for each individual case.

b. Sudden Crosssection Increase

For a sudden cross section increase, the wall forces are given by:

$$F_W = (A_2 - A_1) (p_2 - p_1) \quad (52)$$

Comparing this equation with Equation 25 one finds that Equation 25 is identical with the above equation for an i -value of 2. With this value, we obtain from Equation 29:

$$\tau = \frac{1}{i} \quad (53)$$

c. Constant Area Duct (Supersonic Diffuser)

For a constant area duct with either subsonic or supersonic flow, the factor i must be zero, since no wall forces in flow direction can appear.

With Equation 29

$$\tau = 1 \quad (53a)$$

4. FLOW DIVERGENCE

In the present radial diffuser system (Figure 7), the radial flow must be redirected into individual diffuser channels as schematically shown in Figure 8. Since this redirection of the flow must be accomplished in a more or less abrupt way, it is a source for flow losses. These losses can be accounted for by applying the law of conservation of momentum to the flow. For the ratio of the momentum of the flow in direction of the diffuser channel to the total momentum of the radial flow portion entering the diffuser channel, we can write (for notations see Figure 8).

$$\frac{I_{\text{chan}}}{I} = \frac{\int_{\beta_0}^{x_0} p \cdot \gamma \cdot M_{\text{chan}}^2 \cos^2 \beta \, dx}{\int_{\beta_0}^{x_0} p \cdot \gamma \cdot M^2 \, d(r \cdot \beta)}$$

For small angles, β_0 ($< 10^\circ$) the following approximations apply:

$$x = r \cdot \beta$$

$$\frac{\beta}{\beta_0} = \frac{x}{x_0}$$

$$\cos \beta \approx 1 - \frac{\beta^2}{2}$$

Then the integration yields:

$$\frac{I_{\text{chan}}}{I} = 1 - \frac{\beta_0^2}{3} + \frac{\beta_0^4}{20}$$

$$\approx \cos \beta_0 + \frac{\beta_0^2}{6}$$

For the diffuser entrance Mach number, we can then write:

$$M_{\text{chan}} = M \sqrt{\cos \beta_0 + \frac{\sin^2 \beta_0}{6}}$$

Resulting losses are in general very minor for the cases considered here.

SECTION IV

WALL FRICTION LOSSES IN AN EXPANSION NOZZLE

1. GENERAL CONSIDERATIONS

In applying the common concept of a pipe friction coefficient to a duct of non-cylindrical shape such as an expansion nozzle, two obvious problems arise. One is the choice of the proper flow condition to be entered in Equation 24; the other one is the choice of the proper duct length-to-diameter ratio also occurring in this equation. In the following it will be shown that these problems have a satisfactory solution and that there is no formal difficulty determining the wall friction forces for an expansion nozzle as long as the friction coefficient is a given constant.

2. CHARACTERISTIC FLOW CONDITIONS FOR WALL FRICTION LOSSES

Introducing in Equation 32 the following substitution

$$D_2 = 2\sqrt{\frac{A_2}{\pi}} \quad (54)$$

and by introducing p_0 and the square root of A^* into the equation we obtain:

$$F_f = \left[\gamma M_2^2 \sqrt{\frac{A_2}{A^*}} \frac{p_2}{p_0} \right] c_f \frac{L}{4} p_0 \sqrt{A^*} \sqrt{\pi} \quad (55)$$

For a given gas, the dimensionless expression in brackets is a unique function of the Mach number prevailing in the exit crossection A_2 , in accordance with the relations for isentropic expansion:

$$\frac{A_2}{A^*} = \frac{1}{M} \left[\frac{1 + \frac{\gamma-1}{2} M^2}{\frac{\gamma+1}{2}} \right]^{\frac{\gamma+1}{2(\gamma-1)}} \quad (56)$$

$$\frac{p_0}{p_2} = \left[1 + \frac{\gamma-1}{2} M^2 \right]^{\frac{\gamma}{\gamma-1}} \quad (57)$$

This approach is not quite accurate, since in the presence of wall friction the expansion is no longer isentropic and Equations 56 and 57 need a correction. This could be accomplished by introducing an estimated polytropic expansion efficiency. However, compared to the inaccuracies involved in determining the friction coefficient itself, this effect is small and neglected here.

The magnitudes in Equation 55 outside the brackets are constants for a given expansion nozzle, except the length L which can be chosen freely. If we make L very short in comparison to the total length of the expansion nozzle, we obtain the friction force acting on a short and nearly cylindrical segment of the expansion nozzle at the exit cross-section A_2 . By applying this approach to other cross sections along the expansion nozzle, we obtain the distribution of the local friction force along the nozzle. Figure 9 gives the distribution of the local friction force with the constant magnitudes in Equation 55 set unity, as a function of the square root of A_2/A^* . Plotting F_f against the square root of the area ratio makes the distribution curve identical to the one applicable to a round expansion nozzle with straight contours as drawn in the plot. On the abscissa, the Mach number applicable to the area ratio is also entered in Figure 9.

Within the accuracy of the chosen friction coefficient, the area underneath the distribution curve from the inlet to the exit of the expansion nozzle is a direct measure for the complete friction force acting on the nozzle wall. With the help of this integrated value, the validity of the simplified approach taken in the momentum equation in Section III can be checked. In Equation 32 the reference flow conditions are those at the exit of the nozzle. The L/D in this equation is obtained by dividing the total length of the nozzle by the exit diameter, i.e., the implied assumption is that the friction force is constant along the nozzle. In Figure 9, the distribution for this simplified approach is then represented by a straight line drawn parallel to the abscissa through the exit point on the true distribution curve. Taking as an example the 3.3 Mach number nozzle of the present design and assuming

an inlet Mach number of 0.25, the areas beneath the straight line and the true curve are approximately equal; i.e., both approaches give the same result in this case. This coincidence is accidental. However, the distribution curve in Figure 9 is universally valid and a correction factor can be established for any combination of inlet and exit Mach number. These correction factors are universally valid for any cross-sectional shape of the expansion nozzle (Section IV.3).

With the availability of a universally valid correction system, no formal difficulties exist to obtain correct friction forces with the simplified method introduced here.

The real difficulties for determining friction forces in supersonic expansion nozzles lie with the friction coefficient itself. Wall friction coefficients for supersonic flow are not well established. Besides being a function of the Reynolds number, they depend also on the Mach number itself. In addition, the flow in an expansion nozzle is never the fully developed type of flow normally assumed for standardized wall friction determinations.

The advantage of the present method of wall friction determination in expansion nozzles is that it allows comparative studies of expansion nozzle configurations and provides at least approximate results in the absence of any other simple method.

3. NON-CIRCULAR EXPANSION NOZZLE

The common relation for pipe friction as used here assumes a circular cross section for the duct for which the friction forces should be determined. This restriction is only a formal one. In the basic derivation of the pipe friction relation, this restriction does not even enter since it deals with the concept of the hydraulic radius which is by definition independent of the shape of the cross section. The common pipe friction relation is only a special case of the general relation.

The basic relation for friction on a wall is:

$$F_f = c_W \frac{\rho \cdot v^2}{2} A_W \quad (58)$$

For a cylindrical duct of any cross section shape, the wall surface is

$$A_W = U \cdot L \quad (59)$$

By writing

$$A_W = \frac{U}{A_{cr}} \cdot L \cdot A_{cr} \quad (60)$$

the duct cross section area can be introduced in the relation for the friction force in a duct. The ratio A_{cr}/U is the well known hydraulic radius of the duct:

$$r_{hyd} = \frac{A_{cr}}{U} \quad (61)$$

With this relation Equation 58 can be written:

$$F_f = c_W \frac{\rho v^2}{2} \cdot \frac{L}{r_{hyd}} \cdot A_{cr} \quad (62)$$

This is the basic relation for the friction force in a duct of arbitrary cross section shape. Applying this relation to a circular cross section with diameter δ , by writing

$$r_{hyd} = \frac{\delta^2 \pi}{4 \delta \pi} = \frac{\delta}{4} \quad (63)$$

Equation 62 becomes

$$F_f = 4 \cdot c_W \frac{\rho \cdot v^2}{2} \cdot \frac{L}{\delta} \cdot A_{cr} \quad (64)$$

It is a convention to set

$$4 c_W = c_f \quad (65)$$

calling c_f the pipe friction coefficient.

In terms of this pipe friction coefficient, Equation 62 becomes

$$F_f = c_f \frac{v^2}{2} \cdot \frac{L}{4r_{hyd}} \cdot A_{cr} \quad (66)$$

Thus in any relation previously derived, the friction parameter:

$$c' = \frac{c_f L}{2D} \quad (67)$$

can be replaced by the more general expression with writing $2r_{hyd} = d_{hyd}$

$$c' = \frac{c_f L}{4d_{hyd}} \quad (68)$$

Both equations give the same result for a circular cross section.

For a rectangular cross section which is of particular concern for a ring nozzle system, it is (with small side a and long side b)

$$d_{hyd} = \frac{a}{(\frac{a}{b} + 1)} \quad (69)$$

Equation 66 can then be written:

$$F_f = c_f \frac{\rho v^2}{2} \cdot \frac{L}{a} \left(\frac{a}{b} + 1 \right) A_{cr} \quad (70)$$

The friction parameter is then:

$$c' = \frac{c_f L}{2a} \left(\frac{a}{b} + 1 \right) \quad (71)$$

4. WALL FRICTION COEFFICIENT FOR AN EXPANSION NOZZLE

The prediction of a wall friction coefficient for an expansion nozzle is a complex process. For a straight pipe, the wall friction is already a function of Reynolds number, Mach number, wall surface conditions, and flow history. In case of an expansion nozzle, all these influence parameters change to an appreciable degree from inlet to exit of the nozzle.

The influence of the Mach number on the friction coefficient is not very well established. Since this influence can be considered minor in comparison to those of the other parameters for the accuracies desired here, it is neglected in the present calculations. The flow history is an important factor. Since the flow approaching the ring nozzles is pre-expanded in the perforations of the supply tube (Figure 1) and abruptly dispersed before entering the ring nozzles, it is extremely turbulent and the flow profile development is likely to occur very fast. The large pressure gradients along the flow in the nozzle also promote a fast development of the velocity profiles at each station in the nozzle. For the present calculations, the flow in the nozzle is therefore assumed to be fully developed in a sense that at any local station along the flow path in the nozzle, the velocity profile has the character of a fully developed flow.

The relative wall roughness, given by the ratio of passage diameter over wall roughness height, was estimated to be 500 on the average for the ring nozzles used in the present investigations. As we will see below, this degree of roughness makes the Reynolds number influence nearly constant along the path of expansion in the ring nozzles. To show this, the change of the Reynolds number along the path of expansion will be derived in the following.

One can write for the Reynolds number using the equation of state:

$$Re = \frac{v \cdot d}{\mu} = \frac{P \cdot Y}{R_G \cdot T \cdot \mu} \quad (72)$$

or:

$$\frac{Re}{d} = M \frac{P}{\mu} \sqrt{\frac{Y}{R_G \cdot T \cdot \mu}} \quad (73)$$

This relation can be extended to read:

$$\frac{Re}{d} = M \frac{P}{P_0} \sqrt{\frac{T_0}{T}} \frac{P_0}{\sqrt{T_0}} \sqrt{\frac{Y}{R_G}} \frac{1}{\mu} \quad (74)$$

The pressure and temperature ratio in this relation can be expressed in terms of the occurring Mach number:

$$\frac{Re}{d} = \sqrt{\frac{M^2}{[1 + \frac{\gamma-1}{2} M^2]^{\frac{\gamma+1}{\gamma-1}}}} \frac{P_o}{\sqrt{T_o}} \sqrt{\frac{\gamma}{R_o}} \frac{1}{\mu} \quad (75)$$

assuming μ to be a constant.

With the abbreviation:

$$\alpha = \sqrt{\frac{M^2}{[1 + \frac{\gamma-1}{2} M^2]^{\frac{\gamma+1}{\gamma-1}}}} \frac{\gamma}{R_o} \frac{1}{\mu} \quad (76)$$

Equation 75 becomes

$$\frac{Re}{d} = \alpha \frac{P_o}{\sqrt{T_o}} \quad (77)$$

For air, this relation gives the following values:

M =	1	2	3	3.3
$\alpha =$	2.25	1.33	0.53	0.40

Taking d in Equation 77 as the local hydraulic diameter of the expansion nozzle:

$$\frac{\text{exit area}}{\text{circumfer. of exit}} = d_h = \frac{(2R_n) h}{(2R_n) 2} = \frac{h}{2} \quad (78)$$

we find for the ring nozzles used in the present experiments:

	throat	nozzle exit
$\alpha =$	2.25	0.40
$\frac{h}{2} =$	$0.75 \cdot 10^{-3} \text{ m}$	$2.3 \cdot 10^{-3} \text{ m}$
Re =	$2 \cdot 10^5$	$1.1 \cdot 10^5$

AFWAL-TR-80-3028

From the well known plot of the pipe friction coefficient versus the Reynolds number we find a value of:

$$c_f = 0.02$$

for the pipe friction coefficient at the throat as well as at the nozzle exit. This equality is caused by the wall roughness encountered here which makes the pipe friction coefficient nearly independent of the Reynolds number in the pertinent region.

SECTION V

THE THEORETICAL PERFORMANCE OF A
RADIAL OUTFLOW SYSTEM

1. GENERAL ASPECTS

In determining the theoretical performance of a radial outflow system as schematically shown in Figure 7, only the expansion process is accessible to a realistic treatment. The diffusion process is much too complex to allow any closer performance prediction than that applicable to normal shock pressure recovery. As explained in Section III, the present arrangement for investigating radial flow diffusers relies on the predictability of the expansion performance. In this Section, the results for the Mach No. 3.3 ring nozzle expansion process will be presented with consideration given to the likely accuracy of the calculations.

For the diffuser portion of the flow system only the normal shock recovery for the diffuser inlet flow, which is the same as the expansion exit flow, has been derived. This normal shock performance serves as standard for evaluating diffuser experiments. The present calculations allow the inclusion of wall friction losses in determining the normal shock performance. Results given in this Section demonstrate the comparatively small performance penalty to be paid for subdividing the radial diffuser into many small units exposing a large friction area.

An important subject discussed in this Section is the independence of the present performance calculations from the non-uniformities of the flow. This independence strongly benefits the reliability of the calculations.

2. PERFORMANCE CALCULATIONS

Table 2 provides the design conditions and the analytic performance of the expansion and diffusion process for the Mach number 3.3 ring nozzle system treated in Section II. The first column lists the individual steps in which the calculations proceed. The group of the next seven columns gives the necessary design data together with

immediate derivatives such as the wall force parameter or the hydraulic diameter of the exit cross sections. The applicable equations for determining ϵ for each step of the flow process are listed in the column heading. The next three columns give the results of the performance calculations in terms of expansion Mach numbers, normal shock recoveries with and without wall friction, and expansion pressure ratios. The equations used to obtain these performance data are indicated again in the column headings. For comparison, the performance results for an isentropic expansion process are also listed (see discussion on accuracy).

The essential result for the evaluation of the diffuser experiments is the normal shock pressure recovery ratio 14.24 listed in column 10 for the diffuser without wall friction. Experimental diffuser pressure recovery ratios obtained with the present ring nozzle and cavity arrangement are to be directly compared with above figure for judging the diffuser performance. For supersonic diffusers with a more elaborate geometry than a constant area duct, this comparison figure is not necessarily an upper limit of performance. In general, however, obtaining normal shock pressure recovery with any conventional type of supersonic diffuser is considered a very good performance (Reference 4).

The performance difference in Table 2 for the diffuser with and without wall friction is of basic interest for applying the multi-channel diffuser concept in the present investigations. This concept facilitates the fluid-dynamic design of radial diffusers as explained in the next Section. The performance with wall friction that applies to the conditions of a multi-channel arrangement with a commonly required channel length to hydraulic diameter ratio of 12, is less than 3% lower in terms of pressure recovery as compared to the frictionless diffuser, as a close representation of a diffuser with no subdividing walls. For completeness, it must be mentioned that actual radial flow laser systems would also incorporate a subsonic diffuser. Since subsonic diffusers are not considered a specific problem of the present radial flow system, they have been omitted from these investigations.

3. ACCURACY OF THE PERFORMANCE CALCULATIONS

The analysis provides a standard of comparison for experimental diffuser results. As indicated above, this standard is a sole function of the expansion exit conditions. Two factors influence the accuracy with which these conditions can be predicted. One is the inherent non-uniformity of the expansion flow; the other one is the proper account of the flow losses.

Due to the previously discussed necessity of subdividing the flow expansion system into small units, the expansion flow contains wakes which cause a considerable non-uniformity of the flow entering the diffuser. The nature of the supersonic diffusion process allows a ready account of this non-uniformity. Since the supersonic diffusion process is based on the preservation of the flow momentum, the diffuser inlet conditions need only be interpreted in terms of the flow momentum entering the diffuser. For an experimental determination of this momentum, the impact forces measured with a pitot probe must be integrated over the inlet area. For the analytic determination which is the only one possible as explained before, the flow momentum is an inherent result of the present calculations, which describe the expansion process in terms of the prevailing flow forces (Equation 21). The effective Mach number of the expansion process resulting from the calculations stands as a direct criterion for the integrated exit flow momentum.

For the proper account of the flow losses, it must be considered that the total losses involved are approximately 10% of the available expansion energy (compare column 10 and 14 in Table 2). Two percentage points of this figure, as can be derived from the numbers given in column 9, are due to a sudden change in flow cross section and direction of the flow path (Section III). This influence is a function of the flow geometry and can be readily accounted for. As a result, about 8% of the initial expansion energy is lost due to wall friction which can be determined only with a limited accuracy. The uncertainty is mainly associated with the friction coefficient to which the losses are directly proportional.

AFWAL-TR-80-3028

An estimate of the accuracy of this coefficient is $\pm 20\%$. For the accuracy of the expansion energy at the diffuser inlet follows, then a figure of about $\pm 1.5\%$ or for the expansion Mach number, which is about a square root function of the flow energy, an accuracy of somewhat less than $\pm 1\%$ follows. Roughly the same accuracy applies to the normal shock recovery ratio, the standard of comparison for the diffuser tests.

SECTION VI

RADIAL DIFFUSER DESIGN CONSIDERATIONS

1. THE MULTI-CHANNEL RADIAL DIFFUSER

The flow problem encountered here of diffusing a supersonic, radial flow coming from a cylindrically shaped source with a length to diameter ratio near one or larger, is without a commonly known precedence. Known design considerations for supersonic diffusers have only a limited meaning for the radial diffuser. For example, providing a constant flow cross section for the radial flow by proper contouring of the side walls of the radial flow system not only leads to complex channel geometries but also to intolerable flow conditions, since at desirable L/D ratios of the flow source, strong axial flow deflections become necessary near the walls. Subdivision of the flow becomes an absolute necessity to arrive at reasonable flow conditions for the diffusion process. The subdivision may either be in axial, peripheral, or both directions. Subdivision in only one direction leads to undesirable high aspect ratios of the diffuser channel cross section. The present design provides subdivision in both directions resulting in a multi-channel diffuser (egg-crate diffuser), where each channel can be given a cross section shape with an aspect ratio not larger than two. The subdivision into many small channels allows also a considerable reduction of the radial diffuser diameter since the supersonic diffusion process depends only on a given length to diameter ratio of the individual channel.

The physical justification for applying an extreme of subdivision is the consideration that wall friction losses play only a minor role in the supersonic diffusion process, which operates on the principle of the so-called pseudo shock consisting of a system of supersonic shocks recompressing the flow very nearly in the same degree as a normal supersonic shock. In this shock process which extends for a length of about ten diffuser channel diameters, the channel walls are almost exclusively exposed to subsonic flow conditions only, reducing wall friction to an almost negligible amount. Thus the introduction of wall

surfaces required for subdividing the flow is no deterrent to an effective diffusion process, as long as the Reynolds number of the channel is maintained high enough (above 10^4). The subdivision has functional limitations. For instance, if the diffuser must be cooled, as it is generally necessary for a high energy laser, it may not be possible to effectively cool the wall surfaces in case of a high degree of subdivision. Such considerations are, however, ignored in the present investigations in preference to the general exploration of the behavior of a multi-channel radial diffuser.

2. SPECIFIC DIFFUSER DESIGN CONSIDERATIONS

The present design not only features subdivision in two directions but also in two steps. The flow is first divided axially by parallel plates with beveled inlet edges as seen in the side views in Figure 10 (Section A-A). At the downstream end of these inlet edges, the flow is divided also in peripheral direction by the pie shaped blades seen in the front view of Figure 10. This two-step subdivision is dictated by aerodynamic requirements. The first division provides the channel contraction normally desired for supersonic diffusion. Since, in this contraction region, the flow remains supersonic, wall friction has an essential influence and wall surfaces must be kept to a minimum. The shape of the channel cross section is, on the other hand, not important and can have a high aspect ratio as is the case at the inlet to the diffuser plates. Where the contraction ends and the pseudo shock systems begins, the wall friction becomes unimportant, as pointed out before; but the cross section shape becomes influential and should be near axisymmetric. These conditions are fulfilled by the second division. This design procedure had been previously applied to straight flow supersonic diffusers in Reference 3.

The Multi-channel arrangement allows one to reduce the treatment of the radial flow diffusion to the common problem of the straight diffuser with the exception of the inlet flow. The inlet edges of the diffuser plates are circular arcs and the supersonic flow around these edges must have a pronounced three-dimensional character. The flow area contraction

in the inlet region also has an uncommon shape due to the radial divergence of the flow. Figure 11 shows the area reduction at the diffuser plate inlet plotted over the plate radius related to the inlet radius for the simple wedge-shaped inlet edges used in the present design. The resulting contour nearly has the shape of an inverted supersonic nozzle for parallel exit flow. The utility of this shape for the diffusion process must be found from the experiments. No attempt has been made to analyze these unique inlet flow conditions. Figure 11 also shows the diffuser inlet contour for the theoretical limit of inlet contraction ($M = 3.514$) for the condition that the cross-sectional area decreases linearly with the radius.

3. THE STRAIGHT FLOW SUPERSONIC DIFFUSER

In the following, the general design of the straight channel shock diffuser is discussed. The flow area schedule of the diffuser channel, i.e., the diffuser section downstream of the throat of a supersonic diffuser is determined by two factors: flow stability and performance. The stability requires that it is possible to position the beginning of the shock system very close to the inlet of the channel without the shock system being pushed out of the diffuser by a small disturbance. The channel flow is inherently stable if an upstream movement of the shock system increases the pressure recovery of the diffuser. In this respect a constant area duct is stable with the help of wall friction. If by increasing the back pressure the shock system moves toward the inlet, less supersonic flow is exposed to wall friction and the pressure recovery improves. Thus, the shock system can be moved upstream until the improved recovery balances the new back pressure. Only a new increase in back pressure would further move the shock system upstream and if the increase in back pressure persists, the shock system would be finally pushed out of the diffuser channel.

The flow stability of a diffuser can be increased by giving it a diverging cross section. However, divergence reduces also the overall diffuser performance. Thus, some compromise is necessary to find optimum diffuser conditions. In the following, a graphic method based

on equations previously derived will be shown and this method allows a check on the stability and performance of a diffuser relative to its geometry in terms of its inlet to exit cross-sectional area ratio.

In Section III, the equations for relating the flow conditions in two cross sections of a non-cylindrical duct with wall friction have been derived. These equations can be conveniently used to graphically present the exit condition of a shock diffuser in relation to the inlet condition, the duct geometry, and the wall losses. Equation 45 can be written with the help of Equation 35:

$$\frac{M_2 \left(1 + \frac{\gamma-1}{2} M_2^2\right)^{\frac{1}{2}}}{\gamma M_2^2 \left(\frac{c_f L}{2D} + 1\right) + \tau} = \frac{M_1 \left(1 + \frac{\gamma-1}{2} M_1^2\right)^{\frac{1}{2}}}{\gamma M_1^2 + \tau \cdot t} \quad (79)$$

In this equation, the functional form of the left side, which is given by the exit conditions, is the same as that of the right side, which is a function of the inlet conditions. Thus a graphic presentation of the general function

$$E = \frac{M \left(1 + \frac{\gamma-1}{2} M^2\right)^{\frac{1}{2}}}{\gamma M^2 c + a} \quad (80)$$

once with the coefficients

$$\begin{aligned} c &= 1 \\ a &= t \tau \end{aligned}$$

for the inlet and once with the coefficients

$$\begin{aligned} c &= 1 + \frac{c_f L}{2D} \\ a &= \tau \end{aligned}$$

for the exit gives a set of two curves which correlate inlet and exit Mach number for a duct because the value of E must be the same for the inlet and the exit. Figures 12 through 14 give examples for applying this process to a supersonic diffuser with a diverging, a constant area, and a converging channel. Assuming the inlet Mach number as given, the E -value of the diffusion process is found from the "In"-curve. On the "Ex"-curve, the same E -value determines the exit Mach number at the subsonic branch, since the flow underwent complete shock diffusion. If no shock diffusion would have taken place, the exit Mach number would have been given by the supersonic branch of the Ex-curve. The difference between inlet and exit Mach number in the absence of shock diffusion is then caused by wall friction and flow divergence.

The ratio between inlet and exit pressure can also be determined graphically. Equation 36, which gives this pressure ratio, can be written with the help of Equation 35:

$$\frac{P_{Ex}}{P_s} = \frac{\frac{\gamma M_{in}^2}{\tau \cdot t} + 1}{\frac{\gamma M_{Ex}^2 \cdot c}{\tau} + 1} \quad (81)$$

or in general form:

$$\frac{P_{Ex}}{P_s} = \frac{\frac{\gamma M_{in}^2 \cdot c}{a} + 1}{\frac{\gamma M_{Ex}^2 \cdot c}{a} + 1} \equiv \frac{B_{p-m}}{B_{p-Ex}} \quad (82)$$

where the coefficients for the inlet are

$$c = 1$$

$$a = t \cdot \tau$$

and for the exit

$$c = 1 + \frac{c_f L}{2 D}$$

$$a = \tau$$

The coefficients are identical with those used for plotting the E-curves. Thus any point on an E-curve can be assigned a value given by

$$B_p = \frac{\gamma \cdot M^2 \cdot c}{a} + 1 \quad (83)$$

B_p -values have been marked on the E-curves in Figures 12 to 14.

In accordance with Equation 82 the ratio between two B_p -values belonging to two different E-curves, but having the same E-value, provides the pressure ratio for the flow between the two cross sections represented by the respective E-curves.

To find, for instance, the pressure ratio for our example in Figure 12, we read a value $B_p = 16.7$ at the intersection of the constant E line with the In-curve. On the subsonic branch of the In-curve, we find $B_p = 1.26$. The ratio $B_p/B_p = 13.25$ is then the static pressure ratio between inlet and exit of our diverging diffuser duct.

To check on the stability of the flow, i.e., whether the shock system moves uncontrollably upstream by an increase in back pressure, we investigate the two cases where the shock system starts at the channel inlet and where it starts further downstream. In the second case, we have supersonic flow extending over a portion of the diffuser channel. The pressure ratio across this channel portion is obtained from the B_p values at the intersections of the constant E line with the supersonic branches of the two E-curves

$$B_p = 16.7 \text{ and } B_p = 16.0 \quad \text{then} \quad P_{Ex}/P_{In} = 16.7/16.0 = 1.044$$

The inlet Mach number to the downstream portion of the diverging diffuser channel where the shock system is now located is the exit Mach number of the upstream portion where the flow is supersonic. In Figure 12, we also obtain with this new inlet Mach number a new E-value on the

In-curve and the exit Mach number after complete shock diffusion from the Ex-curve. From the pertinent B_p -values (13.1 and 1.28) we obtain the pressure ratio across the shock system

$$\frac{P_{Ex}}{P_{In}} = \frac{(B_p)_{Ex}}{(B_p)_{In}} = 10.23$$

The overall pressure ratio across the diffuser channel is then $10.23 \cdot 1.044 = 10.68$. We see that this pressure ratio is lower than that resulting for the shock system located upstream. Since the pressure recovery ratio increases with the shock system moving upstream the diffuser is stable.

Table 3 lists all magnitudes of interest derived from Figures 12 through 14 for the diverging, constant area, and converging case. For the converging channel in particular, we find that the pressure ratio for the shock positioned downstream is now higher than when the shock system begins at the channel inlet; i.e., the flow in this converging channel is unstable.

The above considerations about diffuser area scheduling provide the following guidelines for shaping the diffuser.

1. The diffuser should, in the common way, begin with a converging section in which kinetic energy is converted to pressure energy with a minimum of shock losses. The throat of the diffuser is at the end of the converging section.
2. A diverging section should follow the converging section for stabilizing the shock front as close to the throat as possible. Its length should not be greater than necessary for stabilizing the flow.

3. For the remaining length of the shock system, the diffuser duct should be converging again or be at least of constant area.

NOTE: A supersonic diffuser commonly consists of two sections, a converging inlet section and a diverging or constant area section for the shock diffusion process.

Experimental experience can only show the benefits of dividing a supersonic diffuser into three sections as outlined above. Figure 10 gave the design of a radial diffuser plate for the present diffuser tests. In this figure, two versions are indicated; one where the throat is followed by a constant area section and one where one wall of the following section diverges by about 1° . Additional adjustments of the diffuser channel geometry are to be accomplished by epoxy layer built up on the channel walls of the machined diffuser plates.

SECTION VII

CONCLUSION

Supersonic radial outflow expansion systems are afflicted with geometric constraints which make their design and also their operation more complex than is common for straight flow systems. To solve this design problem, design charts have been developed which relate the principal geometry of ring nozzles, the basic elements of the expansion system, to the flow conditions in terms of the isentropic expansion Mach number, weight flow rate, upstream and downstream pressures, and throat Reynolds number. Design charts of this kind have been prepared for four different gases (He, air, CO_2 , and Freon 12). The chart for air has been used to design two radial flow nozzle systems ($M = 2.3$ and 3.3) for use in a test rig to explore radial flow diffusers.

Radial flow diffusers used for laser systems feature unusually large L/D ratios. This geometric condition affects the operation of the diffuser test rig considered here twofold. It requires subdivision of the flow into many small expansion units and prevents the access to the expansion system exit for surveying the flow by means of probes. Subdivision introduces flow losses and simple potential flow considerations are no longer adequate for determining the expansion performance. Since probing of the flow is also not possible, the expansion exit conditions, which are the inlet condition of the diffuser, must be determined analytically with careful consideration of all possible flow losses.

The analytic process which accounts for nozzle wall friction, losses due to sudden flow expansion on the nozzle edges, and the radial divergence of the flow is developed here for a ring nozzle system. For the specific nozzle design to be used for the diffuser test rig, the analysis finds an effective Mach number of $M = 3.514$ (for isentropic expansion $M = 3.688$). For evaluating diffuser test results, the measured pressure recovery is compared to the normal shock recovery pertaining to the effective Mach number indicated above.

For an effective diffusion of the flow in a radial flow system, subdivision of the flow field into small units is necessary. Providing a near constant area flow path as required for supersonic shock diffusion leads to complex flow fields in case of a radial flow field with no subdivision. This is particularly true for the large L/D ratio systems needed for radial flow lasers. Since the walls are exposed only to subsonic velocities in an effective shock diffuser, subdivision poses no flow loss problem as long as the channel Reynolds number does not become too low. Subdivision must be minimized ahead of the diffuser throat, where velocities are still supersonic on the wall (subdivision should be also minimized for any subsonic diffusion following the shock diffusion since there is no longer any inherent need for subdivision in a radial subsonic diffuser). Subdivision can become an operational problem for laser applications where it may interfere with cooling the diffuser.

Subdivision of the radial diffuser into many small units makes it possible to apply a standard geometry to the individual channels. Except for the diffuser inlet where a complex three-dimensional flow field exists, common design considerations apply to the subdivided radial diffuser. Flow stability, which is the principal criterion for the shock diffuser design, is established in a duct if the pressure recovery across the shock system increases when the shock system is moved upstream toward the diffuser throat by increasing the diffuser back pressure. In this respect wall friction makes the flow stable in a constant area diffuser channel. Stability is increased by providing a diverging channel at the expense of the diffuser performance. A possible compromise is to provide a short diversion after the diffuser throat and continue with a constant area channel.

REFERENCES

1. S. Hasinger, "Performance Characteristics of Ejector Devices", Aerospace Research Laboratories, Technical Report ARL TR-75-0205, Wright-Patterson AFB, Ohio, June 1975.
2. S. Hasinger, "Ejector Optimization", Air Force Flight Dynamics Laboratory, Technical Report AFFDL-TR-78-23, Wright-Patterson AFB, Ohio, June 1978.
3. S. H. Hasinger and D. K. Miller, "Two-Dimensional Supersonic Diffuser Experiments", AIAA Journal, Vol. 13, No. 4, April 1975, pp. 536 - 538.
4. D. K. Miller, "Slanted Cascade Diffuser - Feasibility Model Design", Air Force Flight Dynamics Laboratory, Technical Report AFFDL-TR-76-153, Wright-Patterson AFB, Ohio, March 1977.

TABLE 1
GAS PROPERTIES FOR RING NOZZLE DESIGN

Gas	γ	R_g $\frac{\text{Newton m}}{^\circ\text{K Kg}}$	μ $\frac{\text{Newton sec}}{\text{m}^2}$	ϕ $\left(\frac{^\circ\text{K Kg}}{\text{Newton m}}\right)^{\frac{1}{2}}$	$\frac{\phi}{\mu}$ $\frac{\text{m } (^\circ\text{K})^{\frac{1}{2}}}{\text{Newton}}$	$2\pi\mu$ (see μ)	$2\pi\phi$ (see ϕ)
He	1.666	2079	$1.9 \cdot 10^{-5}$	0.0159	838	$11.93 \cdot 10^{-5}$	0.100
47 Air	1.4	287	$1.8 \cdot 10^{-5}$	0.0404	2245	$11.31 \cdot 10^{-5}$	0.254
CO ₂	1.3	189	$1.5 \cdot 10^{-5}$	0.0486	3237	$9.42 \cdot 10^{-5}$	0.305
Prop. 12	1.127	69	$1.3 \cdot 10^{-5}$	0.0764	5879	$8.17 \cdot 10^{-5}$	0.490

TABLE 2
ANALYTIC RESULTS

1	Design Data							Analytic Performance					
	2	3	4	5	6	7	8	9	10	11	12	13	14
Elemental Process of the Radial Outflow System	Elemental area ratio $\frac{A_2}{A_1}$	#1 & #3 Eqs 49 to 51 #2 $\tau = 1/\tau$ (Eq 53) #4 Eq 53a	given by design (see Section III 4)	see Section IV 4	given by design	given by design	Eq 68 $\frac{c_f L}{4d_{hyd}}$	Eq 46 utilizing Eqs 35, 45, 47, & 47a M_2	Eq 36 utiliz. Eq 35 (norm. shock recov.) P_2/P_1	Eq 36 utiliz. Eq 35 (Expans. press. rat.) P_2/P_1	Eq 50 (expans. Mach numb.) M_2	Isentrop. expansion press. ratio for M_2 P_2/P_1	norm. shock recovery for M_2 P_2/P_1
	5.257	0.280	1.0	0.02	11.2	4.60	0.012	3.102		0.5283 0.0393			
	1.061	0.943	0	0.02	0	4.72	0	3.161		0.9132			
	1.449	0.820	3.75	0.02	10.2	29.20	0.002	3.514		0.5774 total: 0.0109	3.688	0.0101	
1. Expansion in the Ring Nozzle System				$c_f = 0$ for #1 to #3									
2. Sudden Expansion at the Ring Nozzle Exit													
3. Expansion in the cavity													
4. Supersonic Shock Diffusion													
without wall friction	1.0	1.0	0	0			0	0.451	14.24				15.70
with "	1.0	1.0	0	0.02	$L/d_{hy} = 12$		0.060	0.461	13.90				

TABLE 3
SHOCK PRESSURE RECOVERY RATIOS FOR 3 DIFFERENT CHANNEL GEOMETRIES

channel geometry	shock position	(B) p In		supersonic branch p _{Ex} /p _{In}		(B) p In		subsonic branch p _{Ex} /p _{In}		total recov. p _{Ex} /p _{In}
		(B) p In	(B) p In	(B) p In	(B) p In	(B) p In	(B) p In	(B) p In	(B) p In	
diverging t = 1.2 (Figure 11)	downstream	16.7	16.0	1.044	13.1	1.28	10.234	10.685		
	upstream	16.7	-	-	-	1.26	-	13.254		
const. area t = 1 (Figure 12)	downstream	18.3	13.5	1.356	13.1	1.345	9.74	13.207		
	upstream	18.3	-	-	-	1.304	-	14.034		
converging t = 0.85 (Figure 13)	downstream	19.6	10.2	1.922	12.6	1.44	8.75	16.818		
	upstream	19.6	-	-	-	1.36	-	14.412		

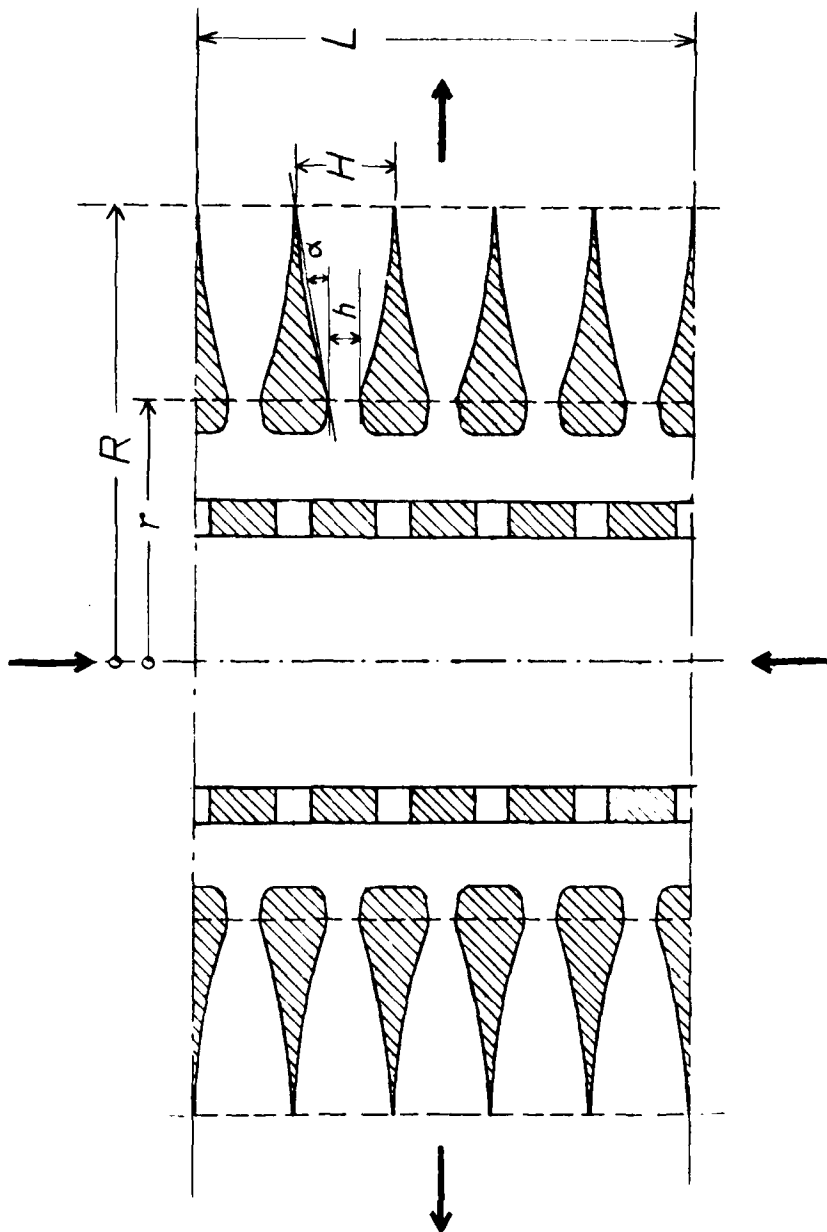


Figure 1. Scheme of a Ring Nozzle Expansion System

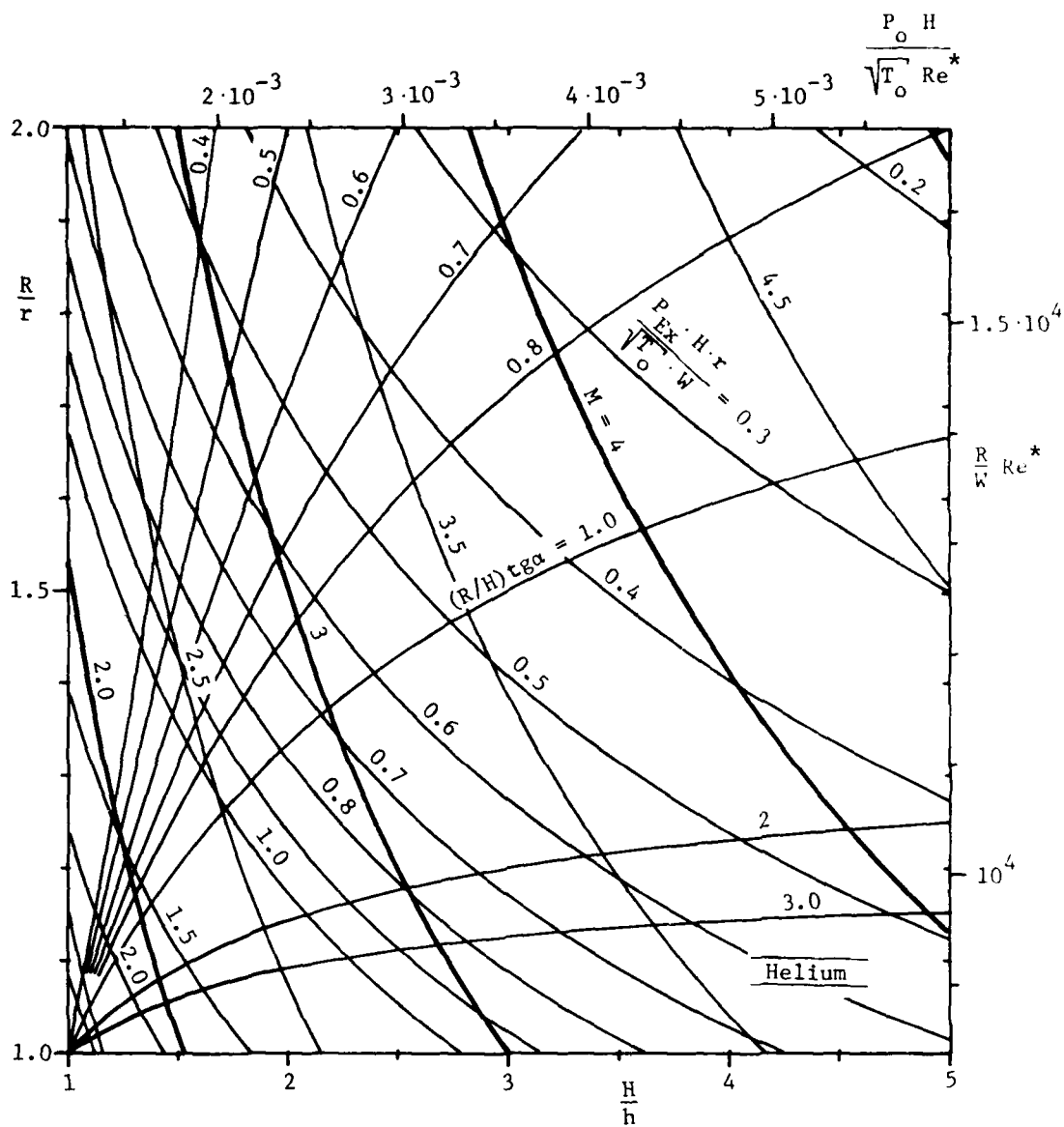


Figure 2. Ring Nozzle Design Chart for Helium. Dimensions:
 P (Newton/m²); H (m); r (m); T (°K); W (kg/sec)

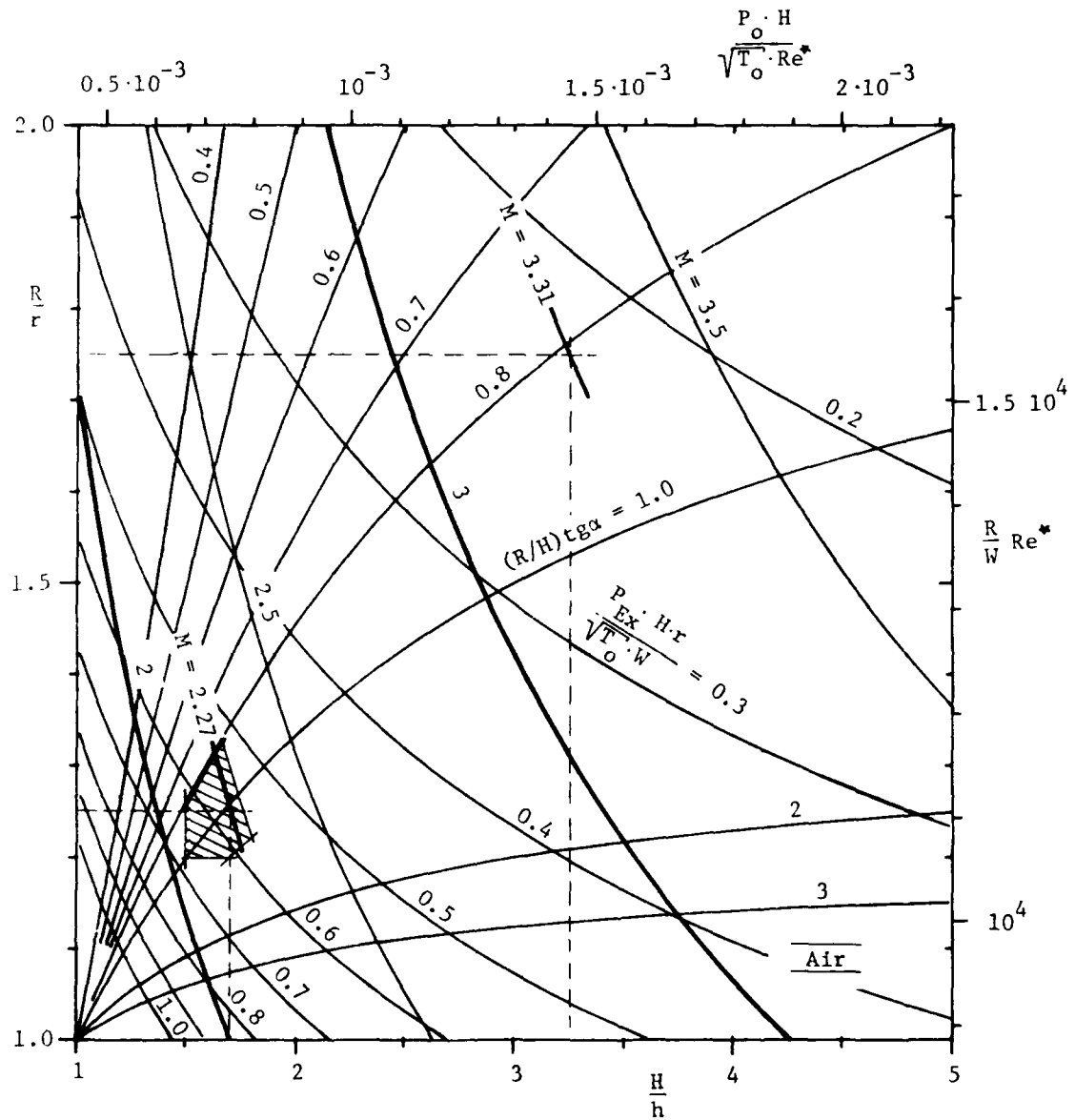


Figure 3. Ring Nozzle Design Chart for Air. Dimensions:
 P (Newton/m²); H (m); r (m); T (°K); W (kg/sec)

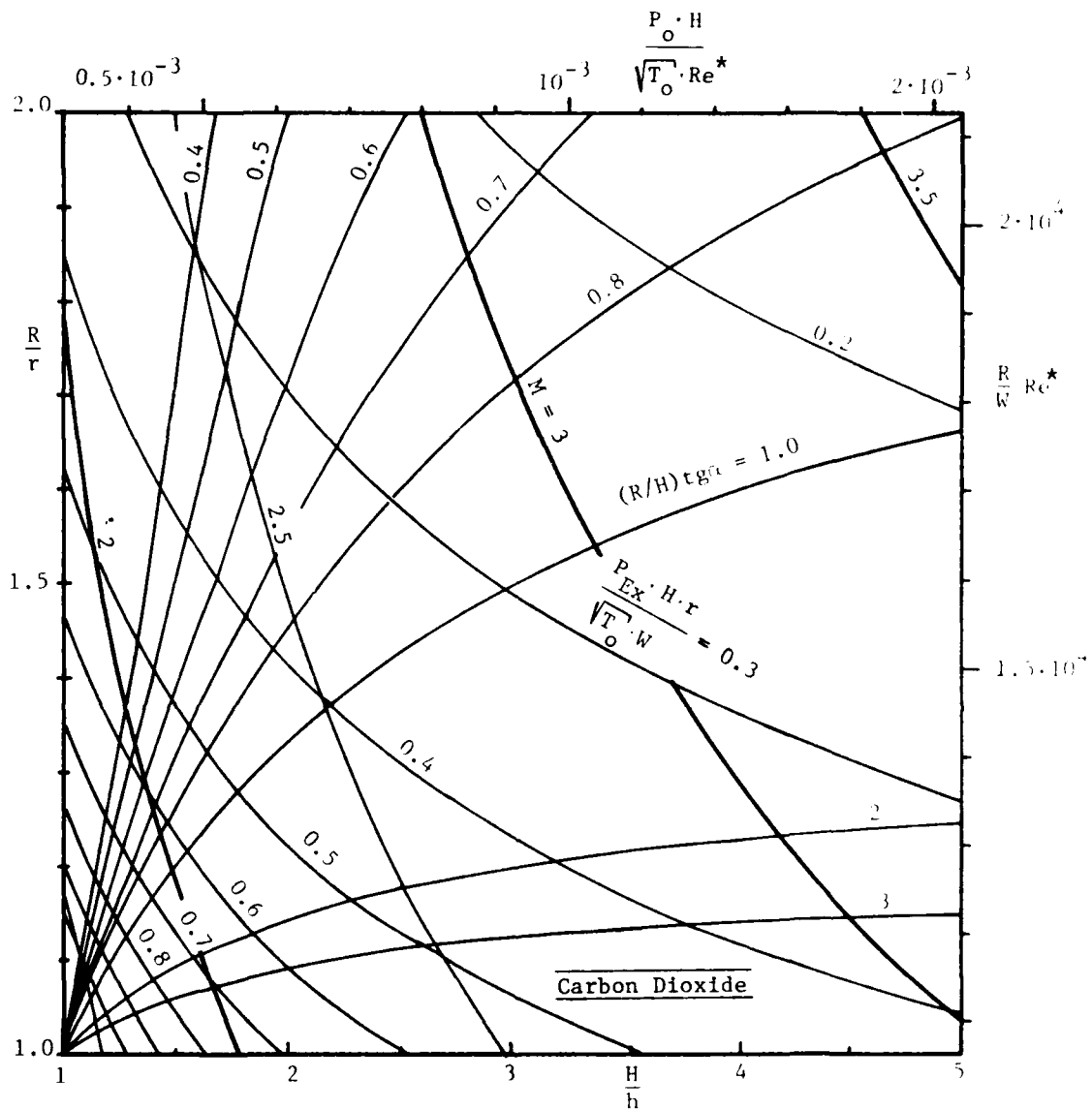


Figure 4. Ring Nozzle Design Chart for CO₂. Dimensions:
P(Newton/m²); H(m); r(m); T(°K); W(kg/sec)

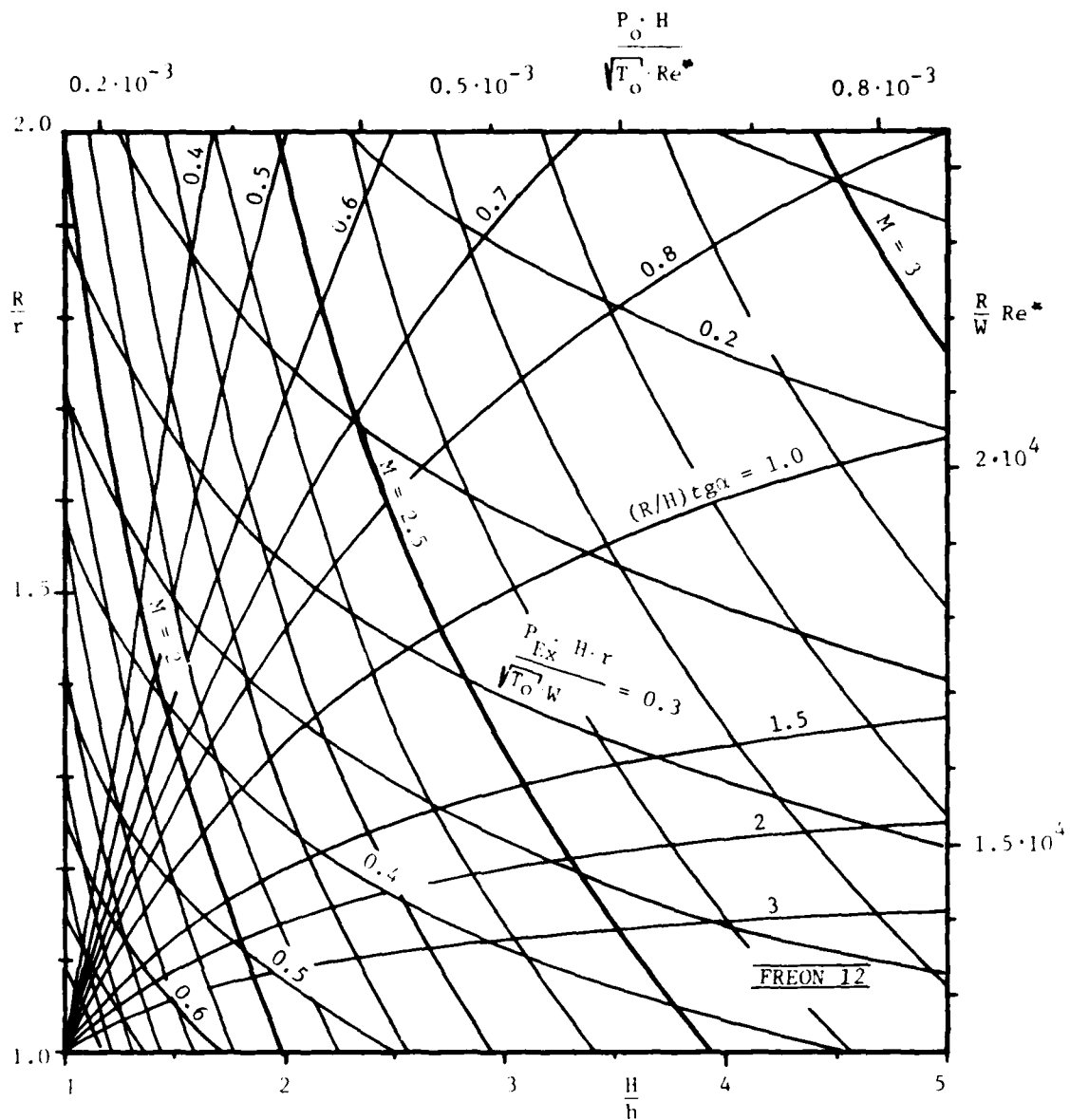


Figure 5. Ring Nozzle Design Chart for Freon 12. Dimensions:
 P (Newton/m²); H (m); r (m); T (°K); W (kg/sec)

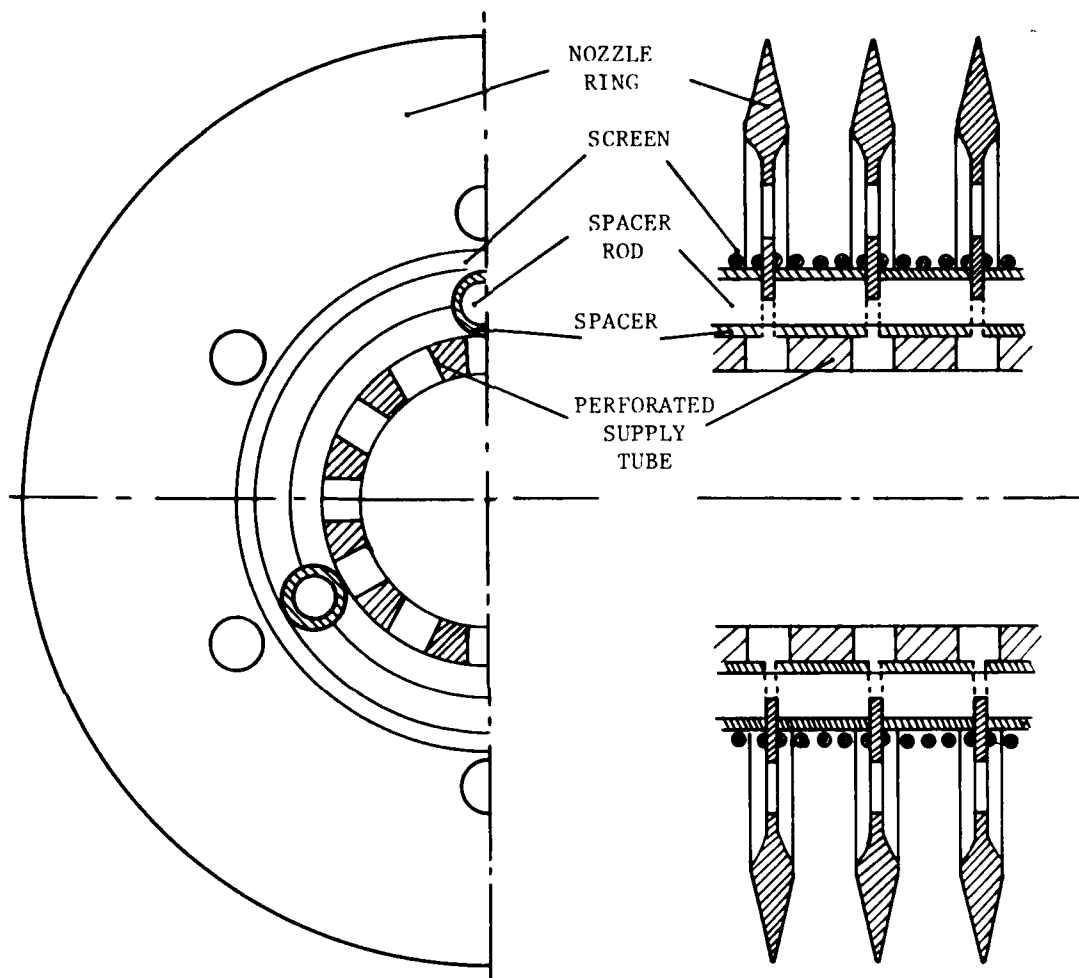


Figure 6. Design of a Ring Nozzle Expansion System for $M = 2.3$

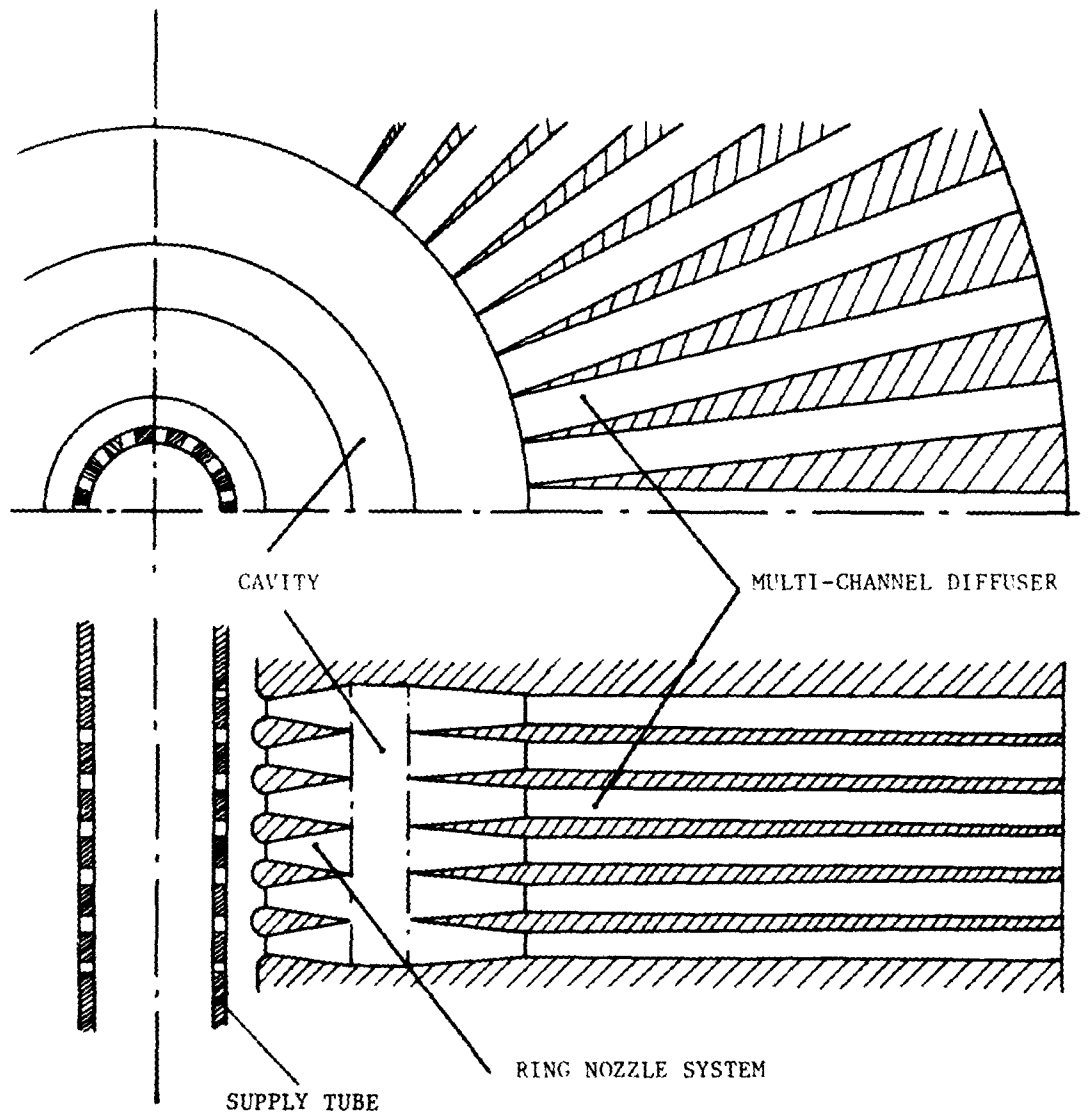


Figure 7. Scheme of a Radial Outflow System

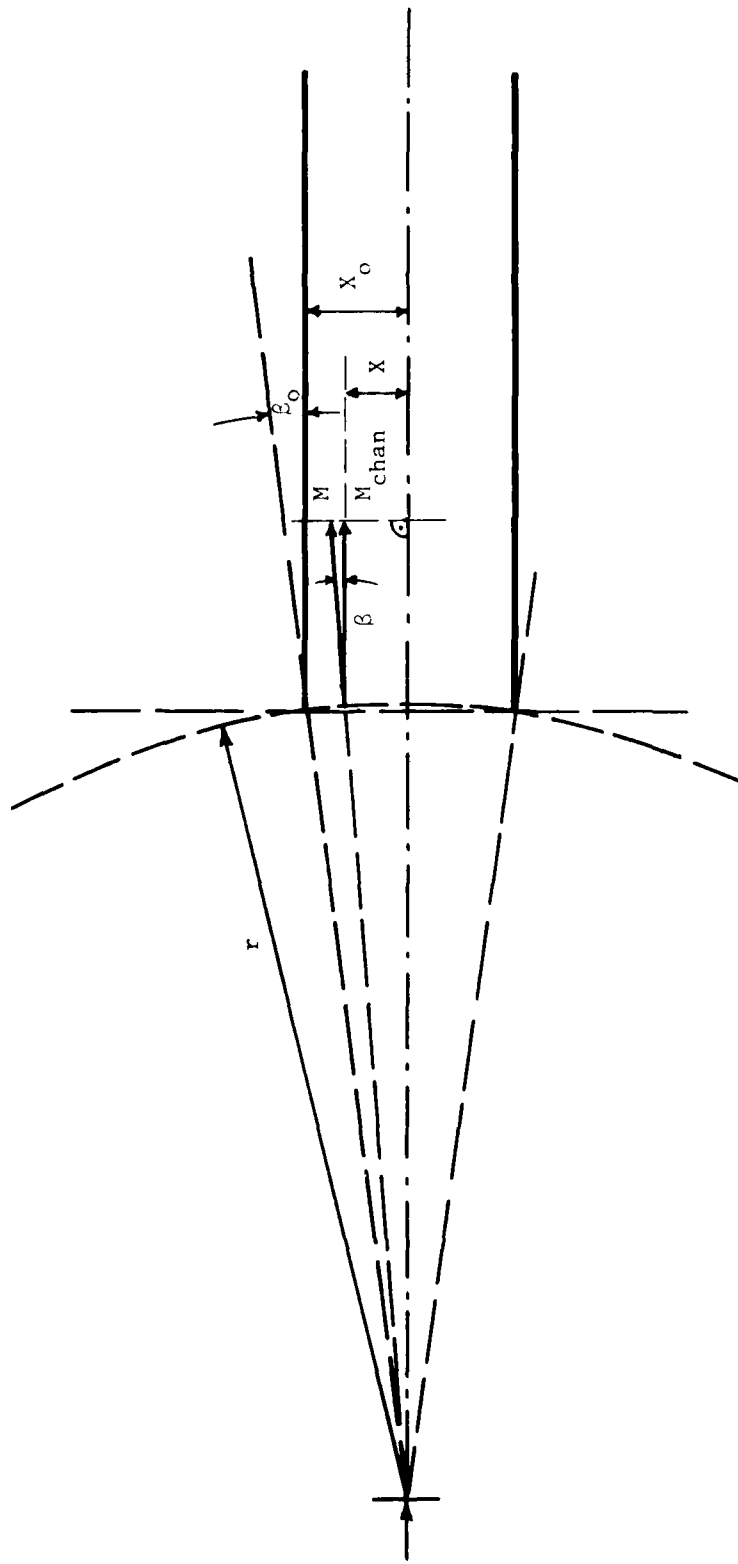


Figure 8. Deflection of the Radial Flow into Individual Diffuser Channel

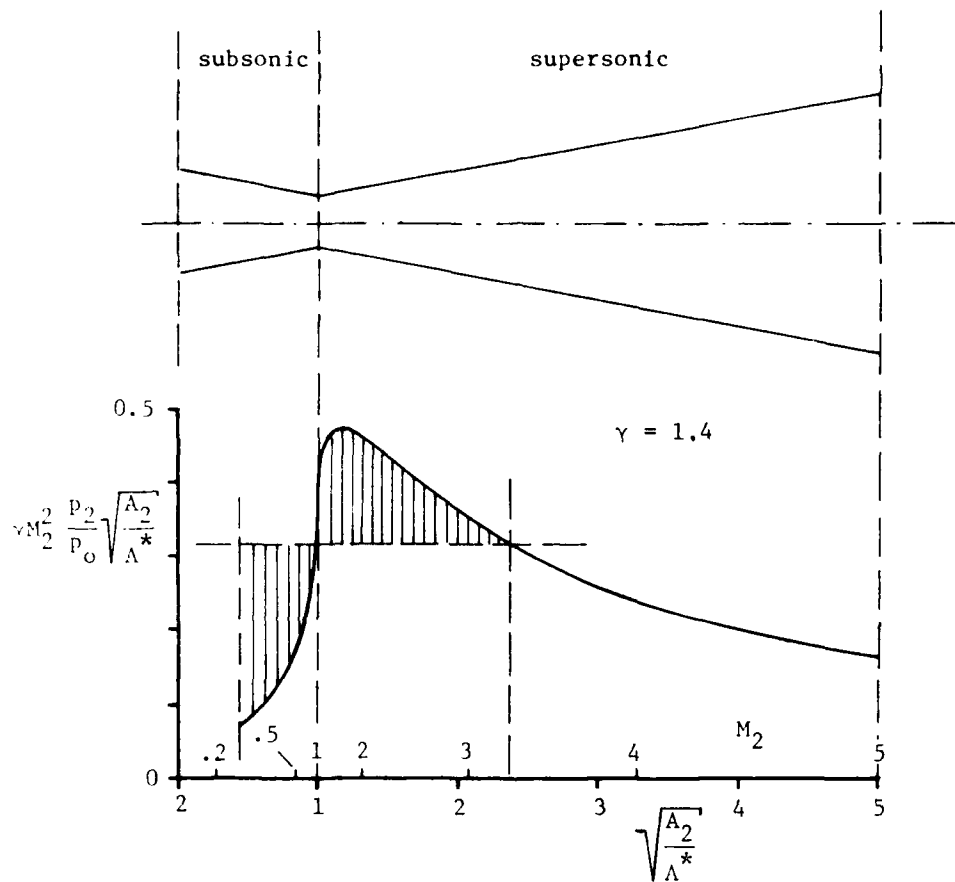


Figure 9. Distribution of the Wall Friction Forces Along a Supersonic Expansion Nozzle for a Constant Wall Friction Coefficient

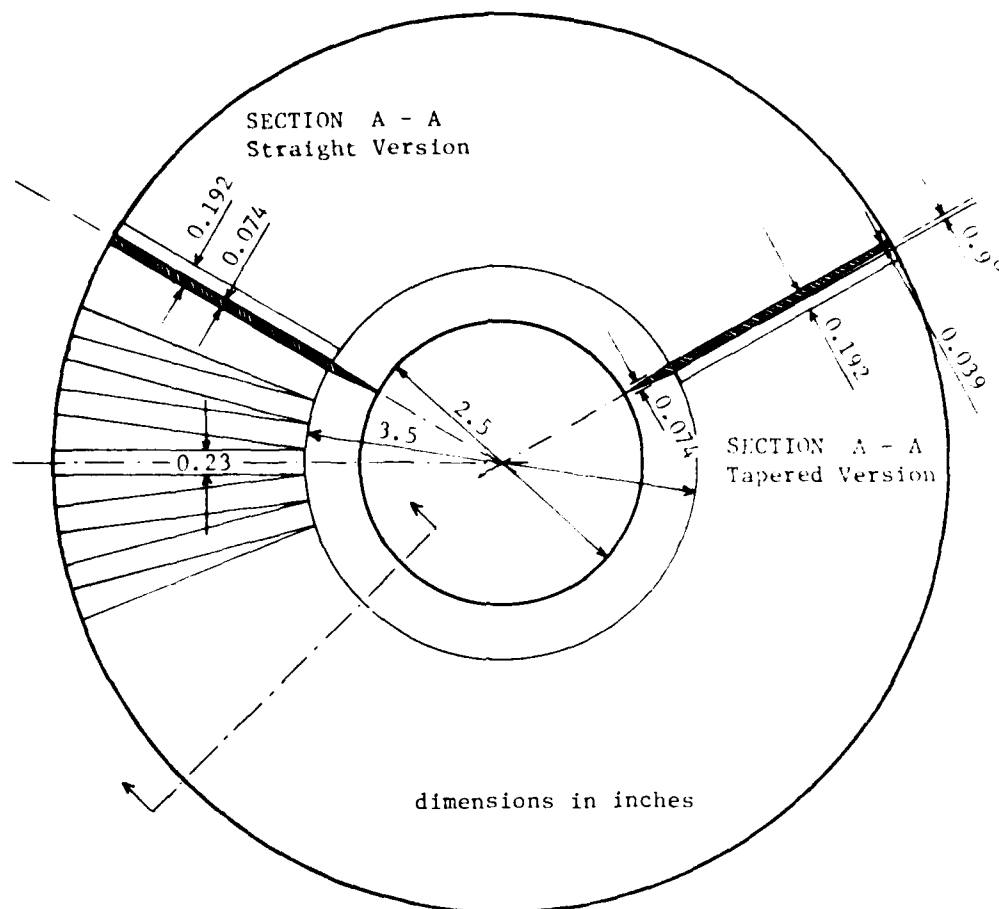


Figure 10. Diffuser Plate Design for a Supersonic Multi-Channel Radial Diffuser

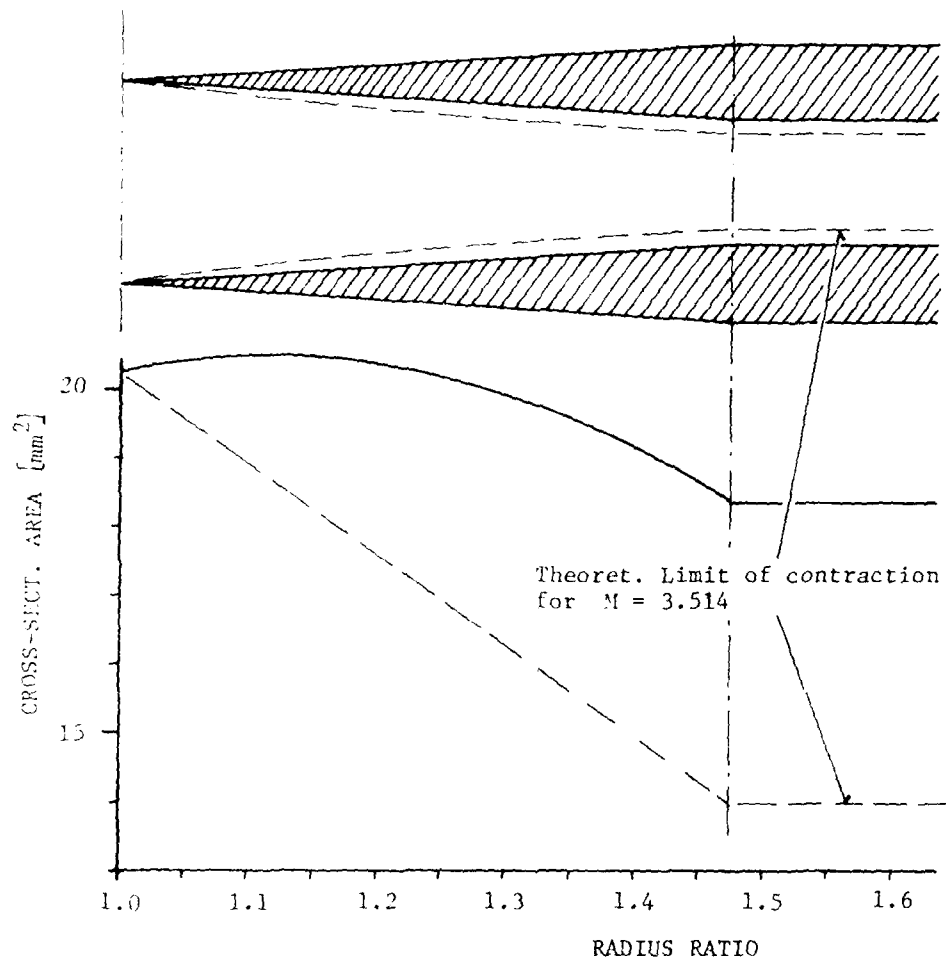


Figure 11. Wall Contour and Cross-Sectional Area for Two Different Radial Diffuser Inlet Geometries. (Wedge shaped inlet (---) is for a throat contraction ratio 0.86; constant rate of inlet area decrease (----) is for a contraction ratio 0.69

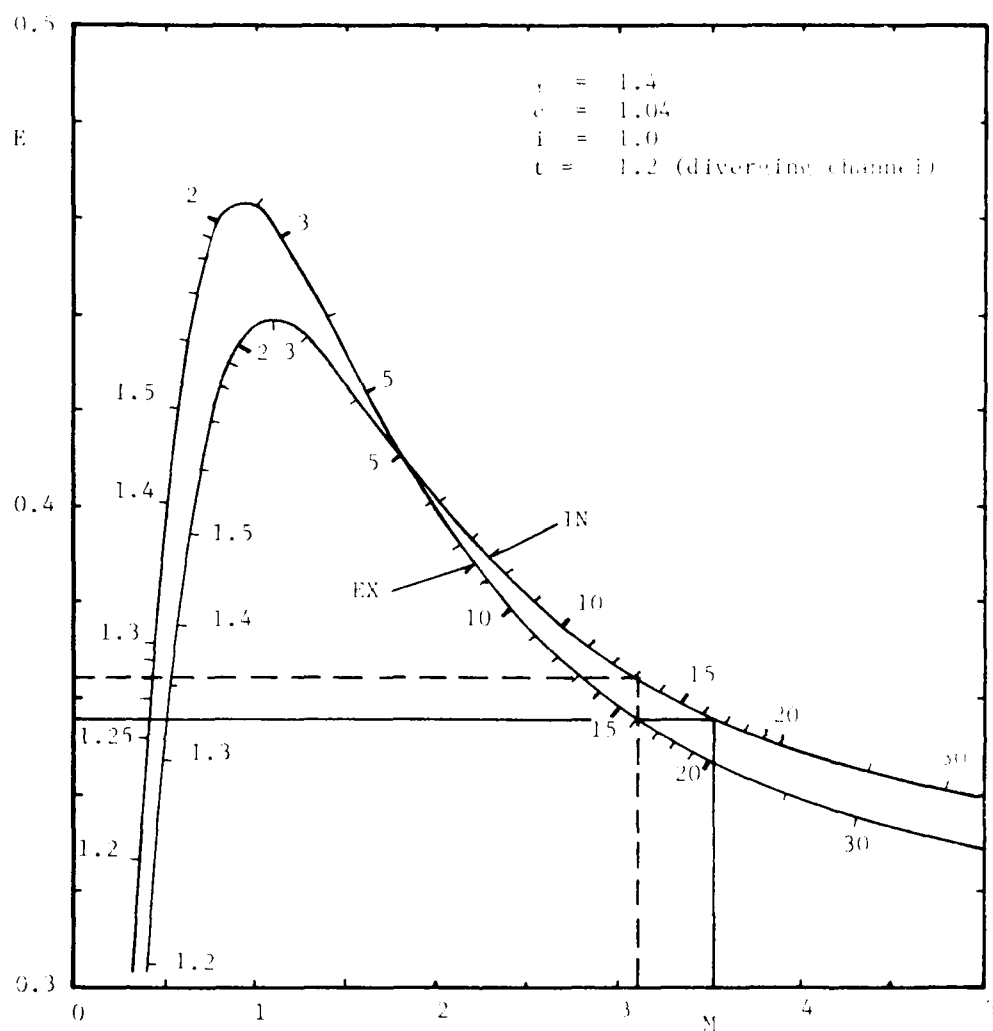


Figure 12. Inlet and Exit E-Function According to Equation 80 for a Diverging Diffuser Channel

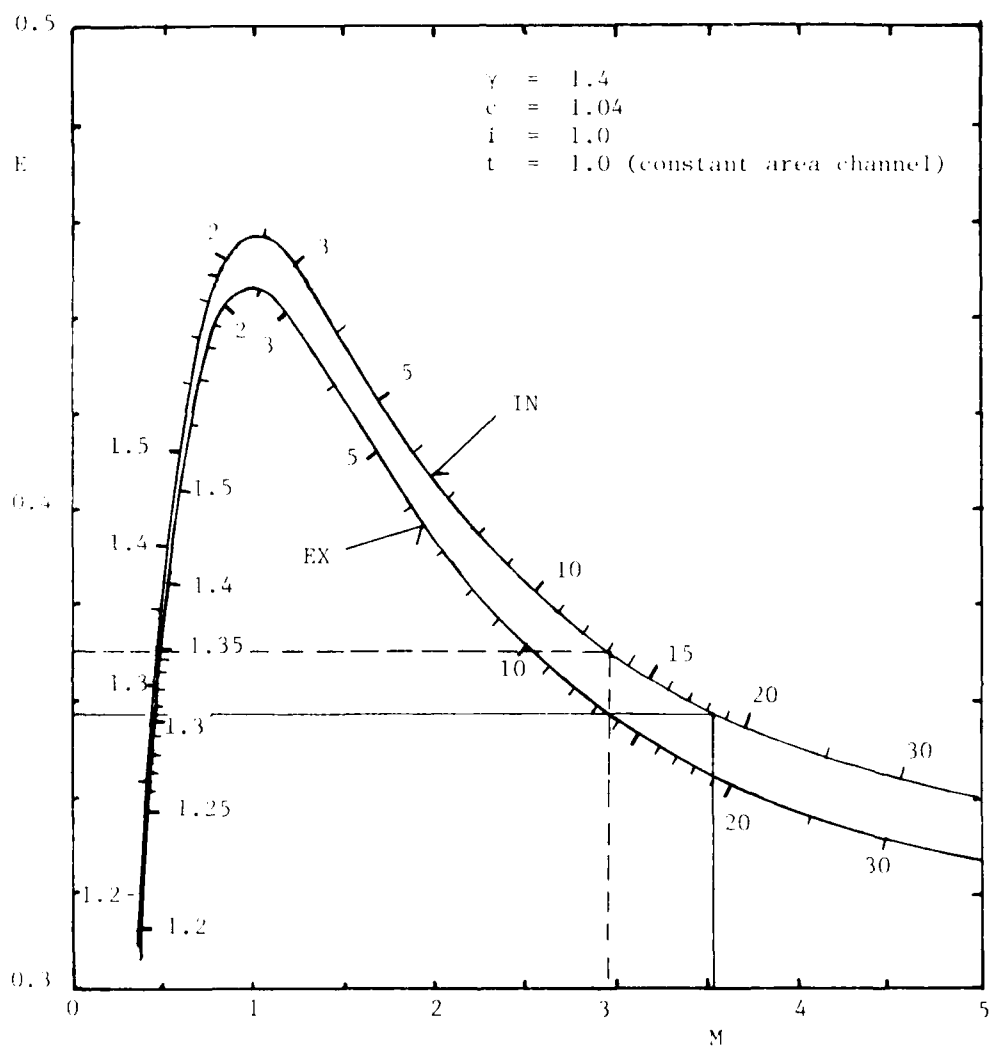


Figure 13. Inlet and Exit E-Function According to Equation 80 for a Constant Area Diffuser Channel

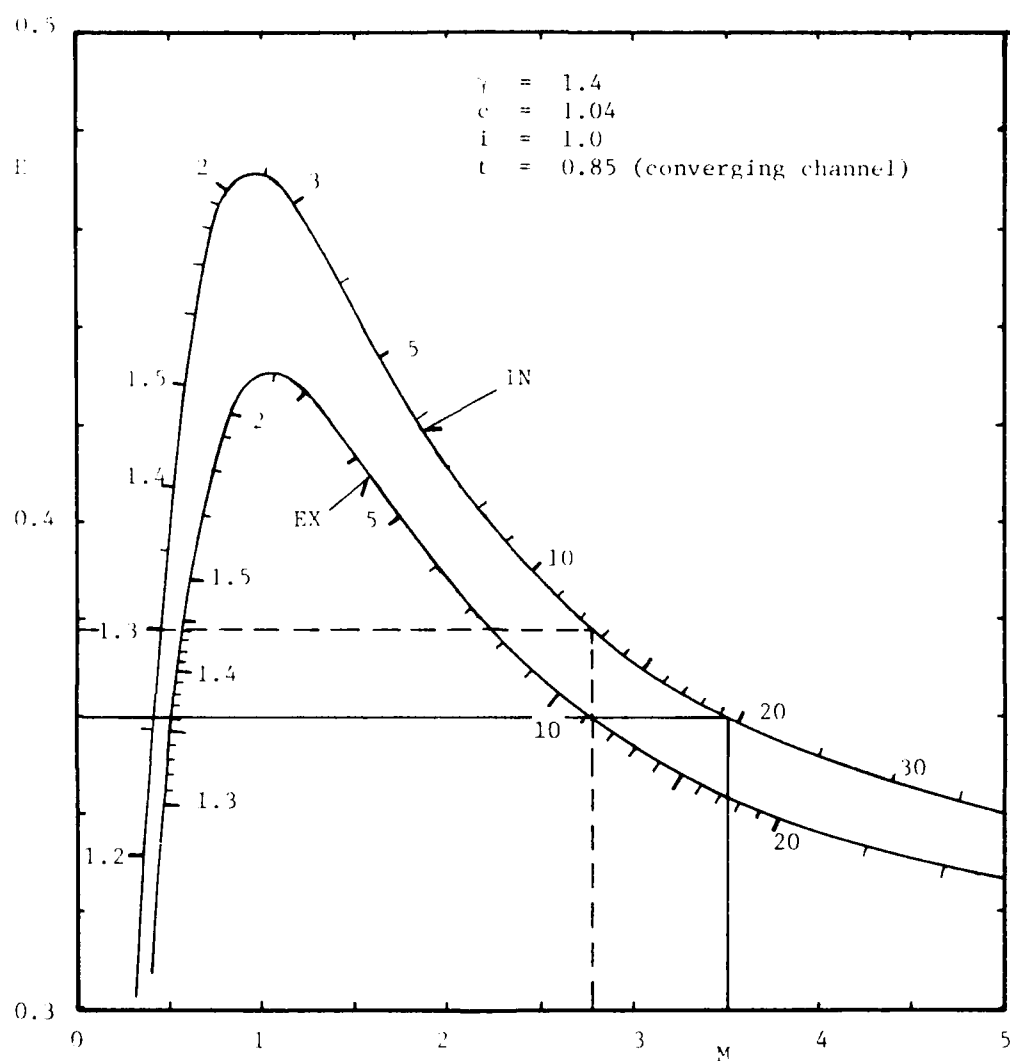


Figure 14. Inlet and Exit E-Function According to Equation 80 for a Converging Diffuser Channel

